

Analysis of the Entropy-guided Switching Trimmed Mean Deviation-based Anisotropic Diffusion filter

U. A. Nnolim

Department of Electronic Engineering, University of Nigeria Nsukka, Enugu, Nigeria

Abstract

This report describes the experimental analysis of a proposed switching filter-anisotropic diffusion hybrid for the filtering of the fixed value (salt and pepper) impulse noise (FVIN). The filter works well at both low and high noise densities though it was specifically designed for high noise density levels. The filter combines the switching mechanism of decision-based filters and the partial differential equation-based formulation to yield a powerful system capable of recovering the image signals at very high noise levels. Experimental results indicate that the filter surpasses other filters, especially at very high noise levels. Additionally, its adaptive nature ensures that the performance is guided by the metrics obtained from the noisy input image. The filter algorithm is of both global and local nature, where the former is chosen to reduce computation time and complexity, while the latter is used for best results.

1. Introduction

Filtering is an imperative and unavoidable process, due to the need for sending or retrieving signals, which are usually corrupted by noise intrinsic to the transmission or reception device or medium. Filtering enables the separation of required and unwanted signals, (which are classified as noise). As a result, filtering is the mainstay of both analog and digital signal and image processing with convolution as the engine of linear filtering processes involving deterministic signals [1] [2]. For nonlinear processes involving non-deterministic signals, order statistics are employed to extract meaningful information [2] [3].

Consequently, image noise filtering is a specialized application area of image processing and research work in this field is vast and constantly evolving. Various filter systems are employed for various types of noise, which exhibit certain characteristics. Examples of such noise types include the Additive White Gaussian Noise (AWGN), Multiplicative (speckle) noise, Poisson noise and impulse noise, etc [1] [2] [3]. The best estimators for the Gaussian noise situation are the averaging or mean filters while the median filters are the ideal estimators for the salt and pepper impulse noise [3]. The rule of filter design is to devise a filter such that its noise suppression ability should not be at the expense of signal (edge) preservation capability. However, this is a contradiction for linear smoothing filters, which have low-pass characteristics [2] [3]. In other words, these filters perform indiscriminate smoothing on both signal and noise. This issue becomes a greater concern with increase in noise levels, where much higher degrees of smoothing are required. This is so due to the eventual over-smoothing of edges in the attempts to suppress or eliminate the noise in the image signal. As noise levels increase, the signal becomes highly degraded with subsequent linear filtering, leading to heavy blurring and/or smudging. Though methods such as using Wiener, Bilateral filtering and Fourier or Wavelet domain-based approaches have been utilized for noise types such as the Gaussian type, they do not work for impulse noise, which has no frequency response [1] for example. Furthermore, the Anisotropic Diffusion algorithm has been successfully applied to the filtering of Gaussian [4] and Speckle

noise [5]. However, we restrict the focus of the work to salt and pepper noise due to the nonlinear nature of the problem and difficulties encountered with high levels of noise.

1.1 Survey of Median-based filters

Median filter and its numerous variants have been shown to be effective at filtering salt and pepper impulse noise. These include the Adaptive Median Filters (AMF) [6] [7] [8], Recursive Median Filters (RMF) [9]- [10], Weighted (stack) Median Filters (WMF) [6], [11], Center Weighted Median Filters (CWMF) [12], Progressive Switching Median Filters (PSMF) [13], Noise Adaptive Fuzzy/Soft-Switching Median Filters (NAFSMF/NASSMF) [14] [15], Fuzzy (Weighted) Median Filters (FMF/FWMF) [16], Median Filtering utilizing Regularization method [17] and Fuzzy FIRE filters [16], [18] to name a few. It is also important to mention the Alpha-trimmed Mean Filter [19]- [20], which is a hybrid filter for filtering impulse noise and additive Gaussian noise depending on the value of alpha parameter.

Some Fuzzy variants utilizing conventional switching schemes [21] [22] [23] [24] [25] [26][18]- [23] use a hard or soft limiter mechanism based on threshold matching the Median Absolute Deviation parameter to gauge the filtering process. However, these work best at low to medium noise density levels and successive application leads to excessive smudging of edges, causing signal degradation. Decision-based and Fuzzy-logic-based filters were developed to address this issue of increased noise density applications [13] [16]. However, these also have a limit in the medium noise density levels, beyond which the fuzzy-based filters fail. Other works have increased the complexity of such median-based filters to address higher density noise situations.

However, these also fail at medium to relatively high levels of noise. Thus, works by [17] and others using Fuzzy Cellular Automata (FCA) [27] have been reported in the literature for improving results. Additionally, trimmed mean filters have also been used for high density impulse noise filtering [28]. As such, there are numerous median-based filters and variants with varying levels of computational and structural complexity and mixed results that it becomes difficult to fully compare all the recent developed algorithms in the literature. However, based on experiments, it can be said that the median filter has reached its limit. Thus, a new approach is required to push the performance of filters for impulse noise filtering.

1.2 Brief overview of Anisotropic Diffusion

Anisotropic diffusion basically involves the modification of the isotropic (equal energy in all directions) heat equation given as shown in (1) [4] [5];

$$\frac{\partial U(x,y,t)}{\partial t} = D \nabla U(x,y) \quad (1)$$

into an anisotropic one where energy is minimized by only allowing diffusion along the edges, resulting in signal preservation [4] [5], yielding the expression in (2);

$$\frac{\partial U(x,y,t)}{\partial t} = \nabla \cdot (D(s) \nabla U(x,y)) \quad (2)$$

In both equations, D is the diffusion coefficient and $\nabla U(x,y)$ is the image gradient. However, the diffusion coefficient is a constant in (1) while it is a varying function of s in (2). The original

functions used by Perona and Malik for D are the Gaussian and Cauchy functions [4] respectively as shown in (3) and (4).

$$D(s) = e^{-\left(\frac{s}{\kappa}\right)^2} \quad (3)$$

$$D(s) = \frac{1}{1+\left(\frac{s}{\kappa}\right)^2} \quad (4)$$

In (3) and (4), $s = |\nabla U|$ while κ is the diffusion threshold parameter [4] [5]. There have been several modifications of the standard approach over the years [29]. One such method proposed a modified diffusion coefficient function obtained by a regularized AD function, in the form [30] shown in (5);

$$s = |\nabla G_\sigma * U| \quad (5)$$

In (5), G_σ is a Gaussian smoothing kernel, with width or standard deviation, σ and $*$ indicates convolution. The modified term is reported to yield a better estimate for local gradient for Gaussian noise [29]. However, the blurring effect, which is a main feature of the regularization operation, is observed. Alternative ways of expressing AD involve using the div operator [29] as shown in (6);

$$\frac{\partial U(x,y,t)}{\partial t} = \text{div}(D(|\nabla U|)\nabla U) = \nabla D \cdot \nabla U + D\Delta U \quad (6)$$

The regularization version as described in [29] is given as;

$$\frac{\partial U(x,y,t)}{\partial t} = \text{div}(D(|\nabla U_\sigma|)\nabla U) = \nabla D \cdot \nabla U_\sigma + D\Delta U \quad (7)$$

Where $U_\sigma(x, y, t) = G_\sigma * U(x, y, t)$ and the diffusion function [29]- [30] is given as

$$D(s) = \begin{cases} \left[1 - \left(\frac{s}{\kappa}\right)^2\right]^2 & \text{if } |s| \leq \kappa \\ 0 & \text{otherwise} \end{cases} \quad (8)$$

Another improved AD formulation [29] is given as;

$$\frac{\partial U(x,y,t)}{\partial t} = \text{div}\left(\left(D(|\nabla U|) - v(|\nabla U|)\right)\nabla U\right) \quad (9)$$

Where $D(|\nabla U|)$ is the diffusion coefficient and $v(|\nabla U|)$ is the sharpen coefficient [29], enabling the expression in (9) to perform simultaneous sharpening and smoothing [29]. The next improved P-M AD model proposed by Sum and Cheung [29] [31] is given as;

$$\frac{\partial U(x,y,t)}{\partial t} = \text{div}(D(|\nabla U|)\nabla U) + \frac{1}{2}|U - U_o| \quad (10)$$

However, as noted in [29], the formulation in (10) does not guarantee robust restoration solution and image edges are not enhanced. Thus, the work of Zhou and Liu [32] goes further by using

not only $U_\sigma(x, y, t) = G * U(x, y, t)$ for the regularization operation but in addition to minimization of energy functional in image domain, Ω [29] [32] given as;

$$E(U) = \int_{\Omega} \rho(|\nabla U_\sigma|) dx dy + \lambda \int_{\Omega} |U - U_o| dx dy \quad (11)$$

Where $\rho(|\nabla U_\sigma|) = D(|\nabla U_\sigma|)|\nabla U_\sigma|$ is the gradient drop flow and $U_o = U(x, y, 0)$, ultimately leading to the gradient flow equation [29] given as;

$$\frac{\partial U(x, y, t)}{\partial t} = \text{div}(D(|\nabla U|)\nabla U) - \lambda(U - U_o) \quad (12)$$

Additionally, Rudin and Osher also proposed the Shock Filter PDE-based model for image enhancement [33][28], which is concerned with sharpening and smoothing. Another popular and well-established PDE-based model is the total variation approach with regularization parameter proposed by Rudin, et al [34]- [35]. However, the standard P-M model yields better edge preservation than the standard TVR method, though there have been improvements based on the works of several authors [29].

With these numerous variations of the original PM AD model, it is important to note that all these are suited to filtering images corrupted with Gaussian noise, though there are few relatively recent works utilizing PDE-based methods for impulse noise filtering [17], [36]- [37]. Additionally, for this work, we slightly modify the equations in order to use the PDE for salt and pepper impulse noise. The proposed algorithm is essentially of two parts, which is common for the PDE-based approaches; namely an impulse noise detector section and a pixel replacement or filtering section. The subsequent sections will discuss both parts in detail.

2. Proposed impulse noise detection and modification filter

We now describe the nature of the first component of the proposed algorithm, which is the Switching Trimmed Mean Deviation Filter (STMDF).

2.1 Switching Trimmed Mean Deviation Filter (STMDF)

Given an ordered set, $X = \{x_1, x_2, \dots, x_j\}$, the trimmed mean, \widehat{x}_m is given as;

$$\widehat{x}_m = \frac{1}{n-2[\alpha n]+1} \sum_{j=[\alpha n]+1}^{n-[\alpha n]+1} x_j \quad (13)$$

Consequently, the sample trimmed median deviation vector is given as;

$$\delta_{STMDF} = \{\widehat{x}_m - x_j\} \quad (14)$$

Additionally, the trimmed mean absolute deviation yields;

$$TMAD = |\widehat{x}_m - X| \quad (15)$$

and the centered trimmed mean deviation yields;

$$\delta_{CTMD} = \widehat{x}_m - x_c \quad (16)$$

Combined with the switching scheme yields;

$$y_c = \begin{cases} x_c; & |\delta_{CTMD}| \leq \tau \\ \widehat{x}_m; & otherwise \end{cases} \quad (17)$$

Where the parameter, $\tau = (\mu_g - \sigma_g) * entropy$ is the entropy guided threshold, while the entropy = $\sum_i^B (-p_i * \log(p_i))$, where p_i is the normalized histogram of the image of bin element, i while B is the total number of bins. Additionally, $\mu_g = \frac{1}{MN} \sum_{m=1}^M \sum_{n=1}^N I(m, n)$ is the global mean while $\sigma_g = \sqrt{\frac{1}{MN} \sum_{m=1}^M \sum_{n=1}^N [I(m, n) - \mu_g]^2}$ is the global standard deviation from the global mean. The local mean and standard deviation could also be used in this expression, though it would considerably increase computation time. The next step is to combine this formulation with the Anisotropic Diffusion filter to guide the filtering along the edges.

2.2 Entropy-based STMDF-Anisotropic Diffusion filter

Following from the work discussed in the introduction, we proceed from the formulation proposed by [5] expressed in the form;

$$\frac{\partial U(x,y,t)}{\partial t} = \nabla \cdot (D \nabla U) + \alpha f(x, y, t) \quad (28)$$

The discretization of the expression leads to the form shown in (29);

$$U^{t+1} = U^t + (\nabla \cdot (D(s) \nabla U) + \alpha f(x, y, t)) \Delta t \quad (29)$$

In (28) and (29), $f(x, y, t) = \text{MedFilt}(U(x, y, t))$, while $D(s)$ is the Cauchy function in (3) and for the proposed approach, we also ensure that the diffusion threshold, κ is computed as a function of image statistical parameters in the form;

$$\kappa = \frac{\mu}{\sigma} \quad (31)$$

Multiplying through by Δt and setting $\Delta t = 1/4$ and $\beta = \alpha/4$ as shown in [23] we obtain the expression in (30), which is the proposed approach where $f(x, y, t) = \text{STMDF}(U(x, y, t))$.

$$U^{t+1} = (1 - \beta)U^t + [\nabla \cdot (D(s) \nabla U)]/4 + \beta f(x, y, t) \quad (30)$$

This enables the computation of the continuous image.

2.3 Total Variation Regularized (TVR) STMDF

Another alternative was using the TVR approach similar to [34].

$$\frac{\partial U(x,y,t)}{\partial t} = \nabla \cdot \left(\frac{\nabla U}{|\nabla U_\epsilon|} \right) + \lambda(U_o - U) \quad (31)$$

Where $U_o = U(x, y, 0) = U_o(x, y)$, which is the initial noisy image and $|\nabla U_\varepsilon| = \sqrt{U_x^2 + U_y^2 + \varepsilon^2}$ is the norm where

$$U_x = \frac{\partial U(x,y)}{\partial x}; U_y = \frac{\partial U(x,y)}{\partial y} \quad (32)$$

Leading to the discrete form;

$$U^{t+1} = U^t + \left[\nabla \left(\frac{\nabla U}{|\nabla U_\varepsilon|} \right) + \lambda(U_o - U) \right] \Delta t \quad (33)$$

With

$$\nabla \left(\frac{\nabla U}{|\nabla U_\varepsilon|} \right) = \frac{(U_x^2 + \varepsilon^2)U_{yy} + (U_y^2 + \varepsilon^2)U_{xx} - 2U_x U_y U_{xy}}{(U_x^2 + U_y^2 + \varepsilon^2)^{3/2}} \quad (34)$$

With $U_{xx} = \frac{\partial^2 U(x,y)}{\partial x^2}$; $U_{yy} = \frac{\partial^2 U(x,y)}{\partial y^2}$; $U_{xy} = \frac{\partial^2 U(x,y)}{\partial x \partial y}$ and ε is a very small number to prevent division by zero. The initial formulation works well for additive and speckle (multiplicative noise). Thus for impulse noise, we reformulate the expression as;

$$\frac{\partial U(x,y,t)}{\partial t} = \nabla \left(\frac{\nabla U}{|\nabla U_\varepsilon|} \right) + \lambda(f - U) + \alpha f \quad (35)$$

Leading to the discrete form;

$$U^{t+1} = U^t + \left[\nabla \left(\frac{\nabla U}{|\nabla U_\varepsilon|} \right) + \lambda(f - U) \right] \Delta t + \alpha f \quad (36)$$

As in (28) - (30), expression in (35) - (36) the term, $f(x, y) = STMDF(U(x, y))$. However, this method does not perform well and needs a kernel of size 7×7 for reasonable results, based on extensive experiments. The approach was abandoned due to sheer computational effort with marginal results. The Anisotropic Diffusion appears to be better suited to the problem than the TVR formulation. So far all AD-based methods have surpassed TVR-based median filter approaches. Median-based STMDF preserves edges better reducing global blurring but yields lower PSNR, especially at higher noise densities while the trimmed mean-based STMDF blurs images, but yields higher PSNR, especially at higher noise densities and coupled with the Gaussian edge-preserving function rather than the Cauchy function.

The choice of using default 3×3 spatial neighbourhoods for both STMDF and AD makes the design stable. Increasing the window size leads to considerable blurring, loss of edge information and details with high degree of smudging. The following section deals with experiments to verify the theoretical formulations and justifications used to develop the proposed approach.

3 Experiments and results

This section presents the image data, the prior experiments aimed at estimation of image statistical parameters and their relationships with regards to noise to enable a more accurate function for noise estimation and detection. Fig. 1 shows the sample images used for experiments while Fig. 2 shows the various plots relating the image parameters to noise density.

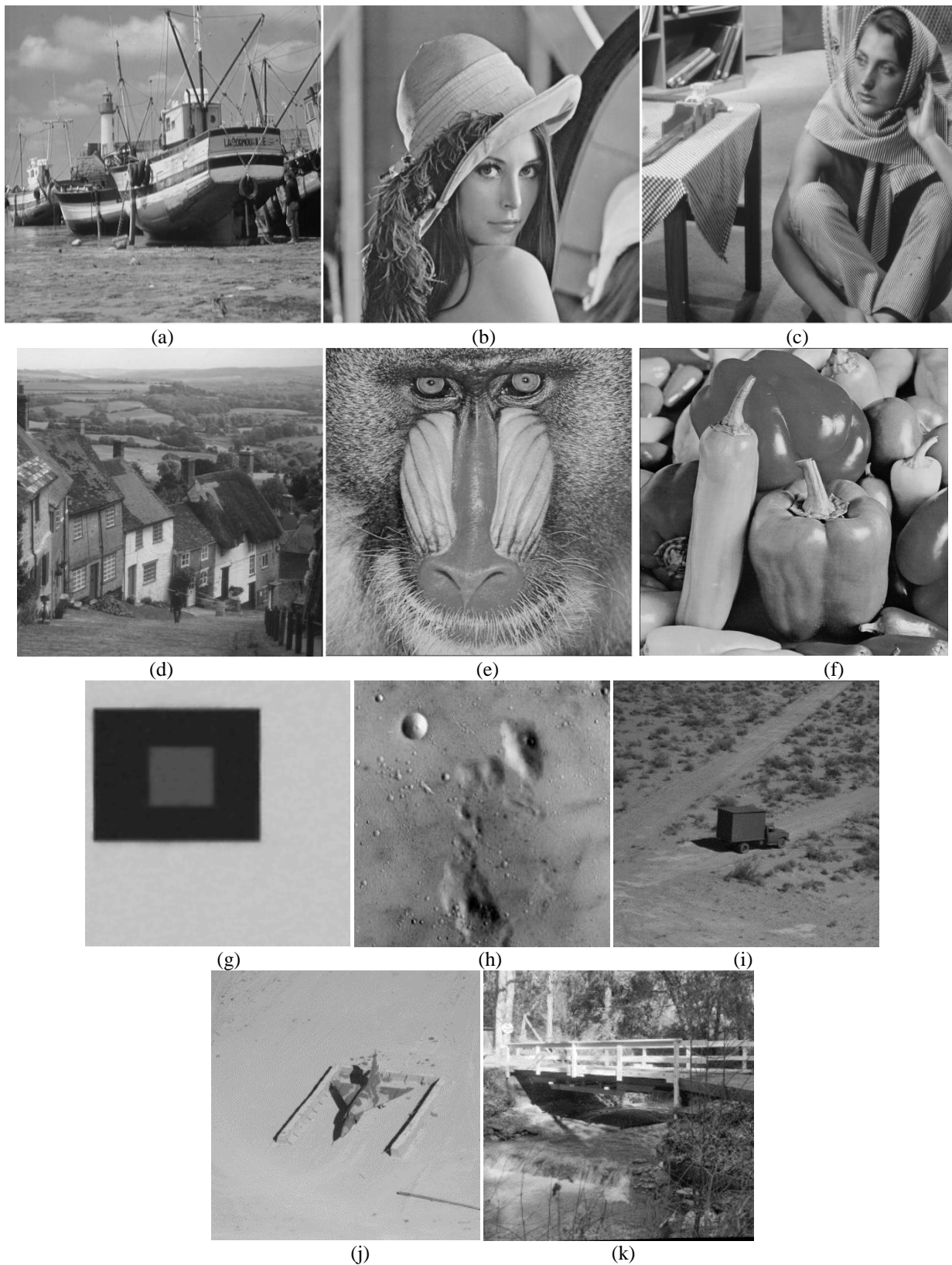
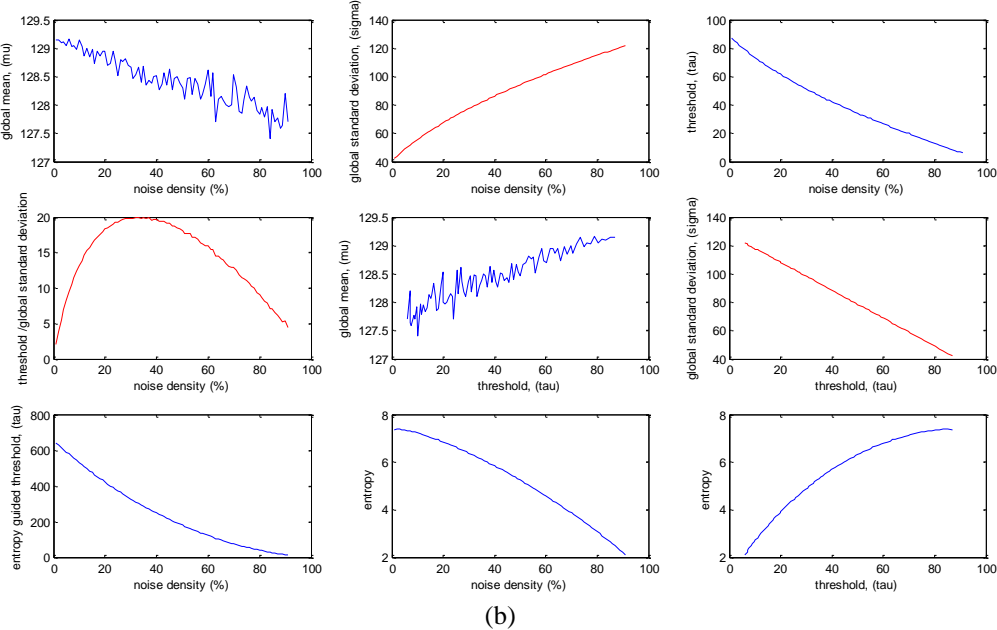
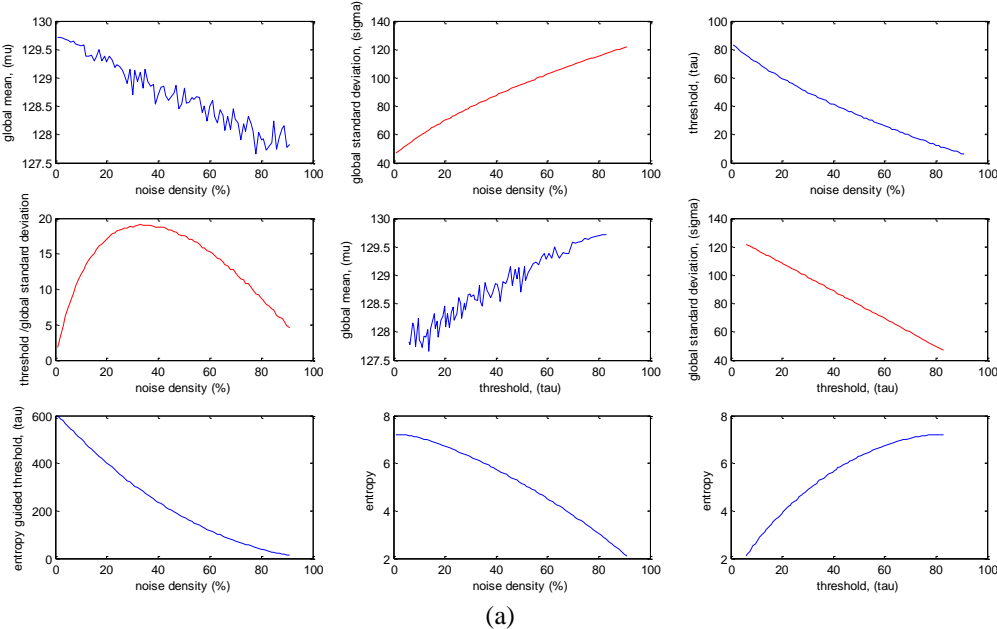
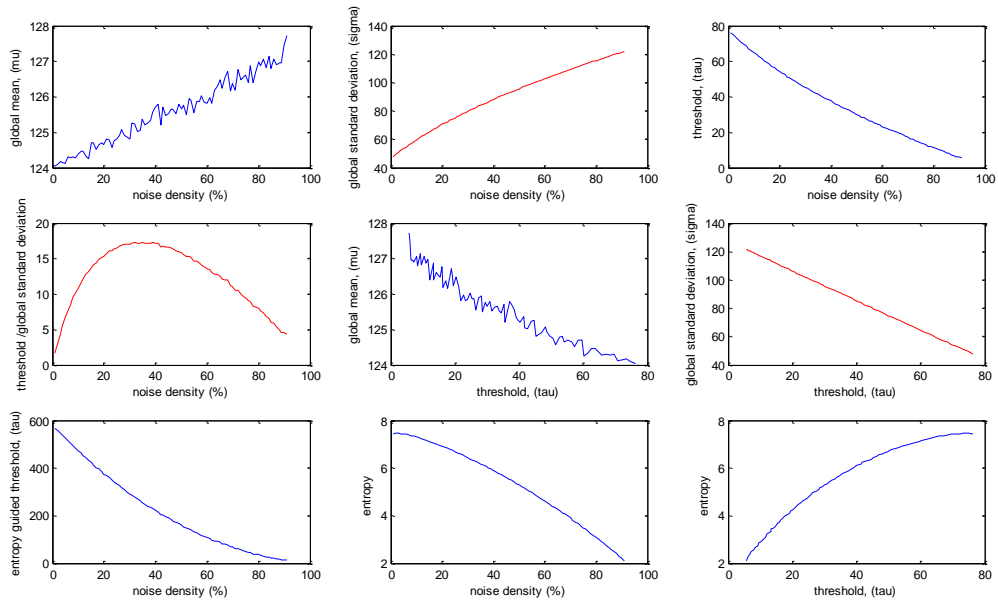


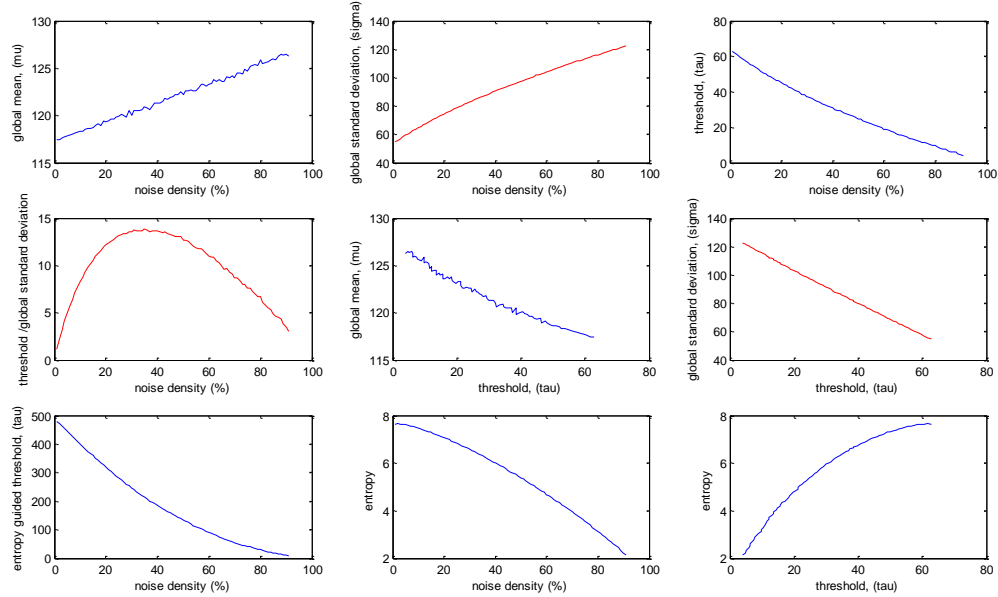
Fig. 1 8-bit sample greyscale images used for experiments: (a) Boat (b) Lena (c) Barbara (d) Gold Hill (e) Baboon (f) Peppers (g) Chip (128×128) (h) Moon (256×256) (i) Truck (k) Jet (f) Bridge (512×512)

The problem is to determine the best function that relates the standard deviation, threshold, entropy to yield a more accurate noise density estimate. Numerous images were tested and the graphs obtained were mostly consistent. In the plots, the most reliable predictors of noise density trends tend to be the standard deviation and entropy parameters. The mean appears to be the least reliable predictor/estimator of noise density, and appears erratic, unstable and unreliable as a noise estimation parameter.

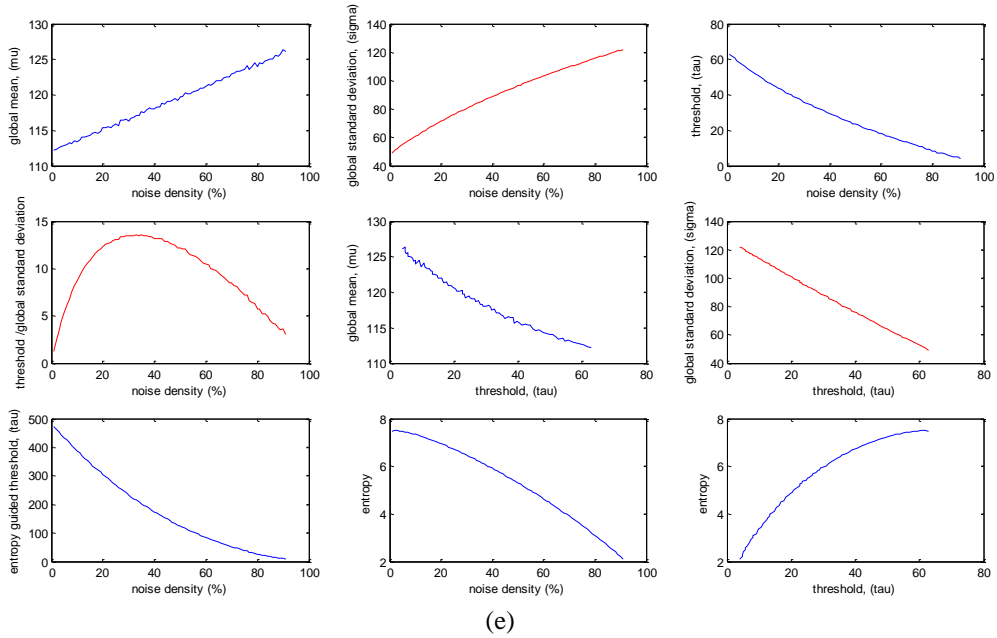




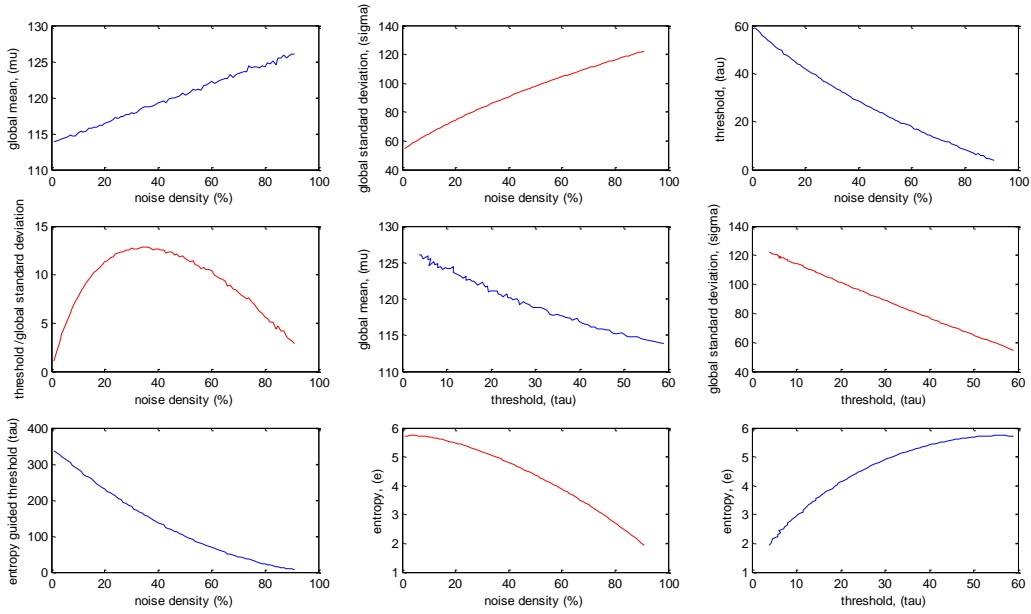
(c)



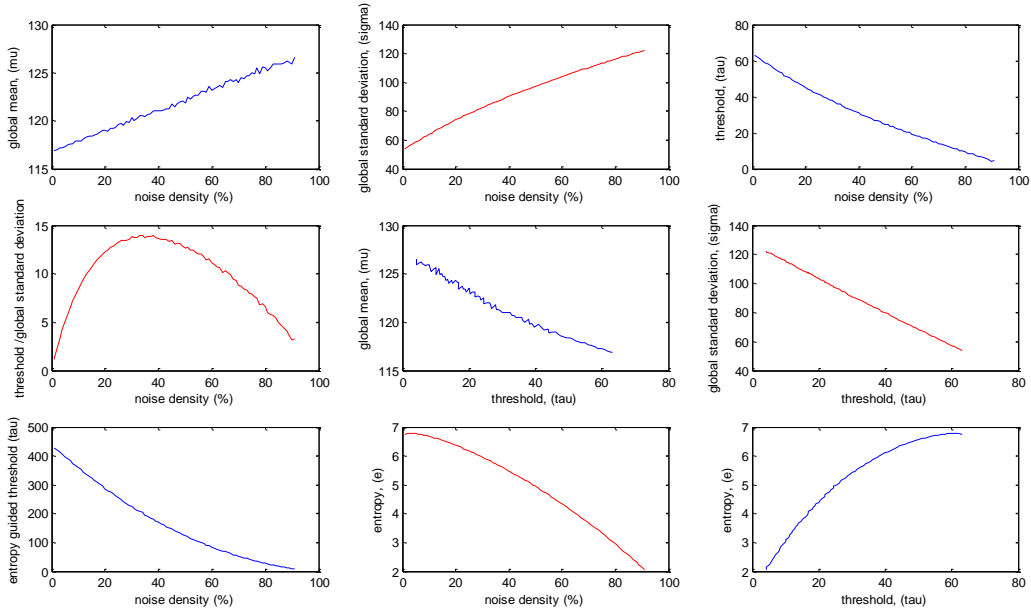
(d)



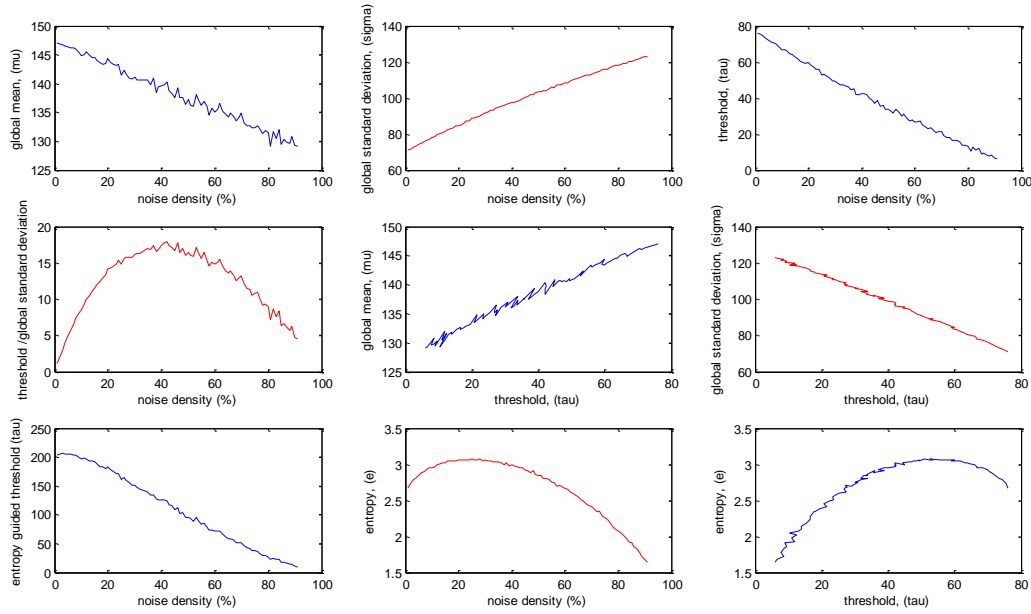
(e)



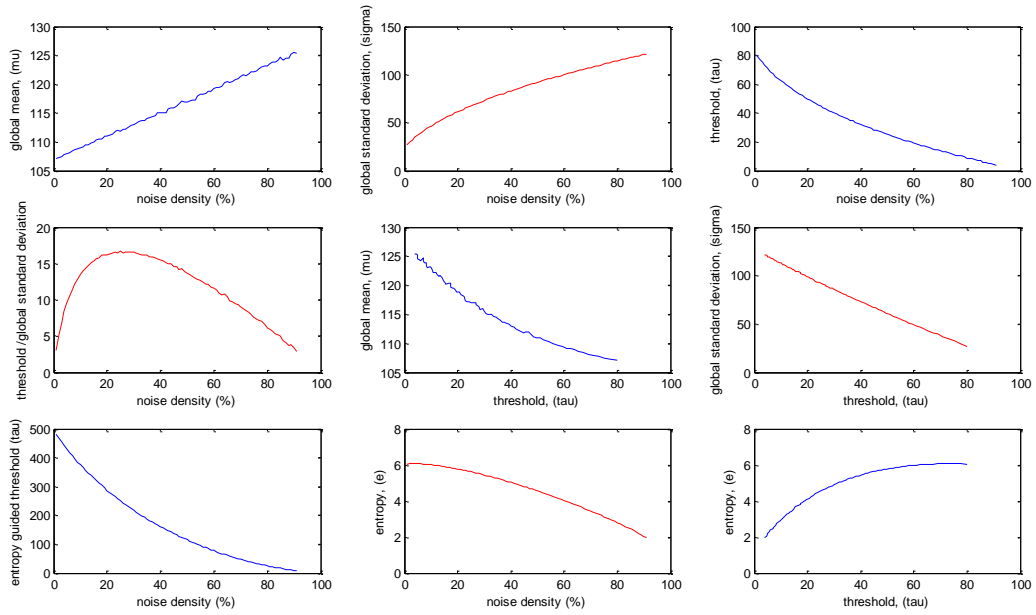
(f)



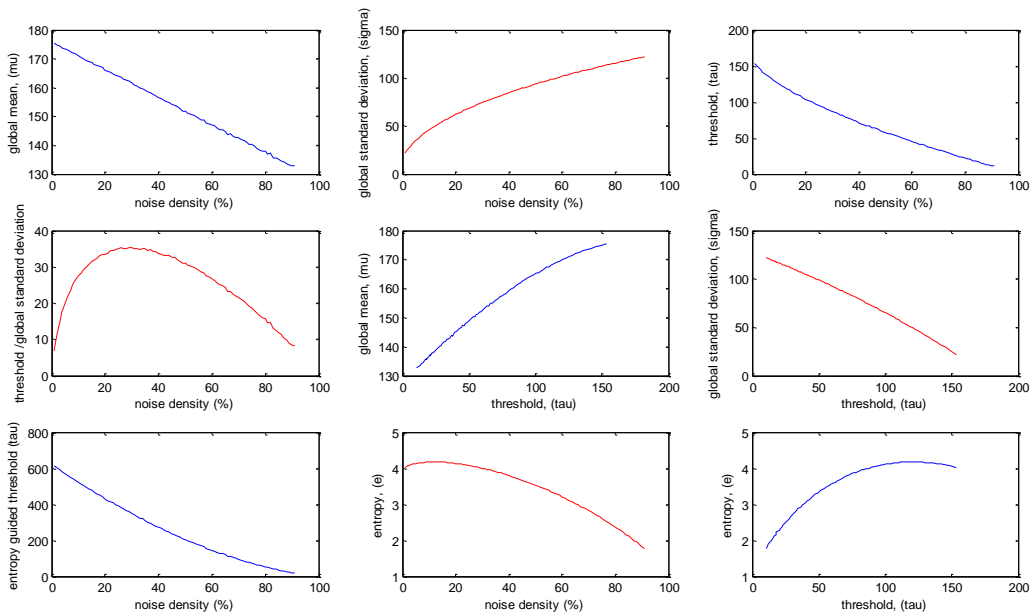
(g)



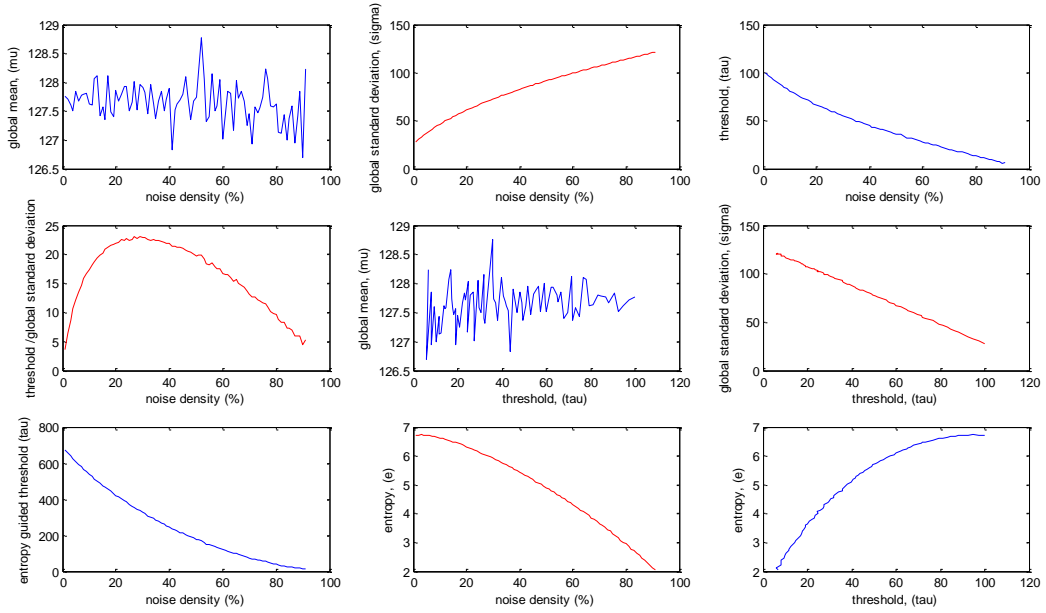
(h)



(i)



(j)



(k)

Fig. 2 plots of image attributes for (a) Boat (Entropy = 7.1914) (b) Baboon (Entropy = 7.3579) (c) Lena (Entropy = 7.4455) (d) Barbara (Entropy = 7.6321) (e) Gold Hill (Entropy = 7.4778) (f) Bridge (Entropy = 5.7056) (g) Peppers (Entropy = 6.7624) (h) Chip (Entropy = 2.6725) (i) Truck (Entropy = 6.0274) (j) Jet (Entropy = 4.0045) (k) Moon (Entropy = 6.7093) images

Initially, experiments were performed with the median filter-boosted anisotropic diffusion. However, the results were unacceptable, especially at high noise densities. This can be seen in Fig.3 and Table 1 showing that a great deal of information is lost and thus, the MF-AD cannot recover much of the original image at high noise densities. At a lower noise density of 50%, five iterations yield some image restoration, which is quite poor compared to results obtained from other median filter variants from the literature. We also utilize a NASMF-boosted AD to compare results and this formulation still did not yield much improvement at higher densities.

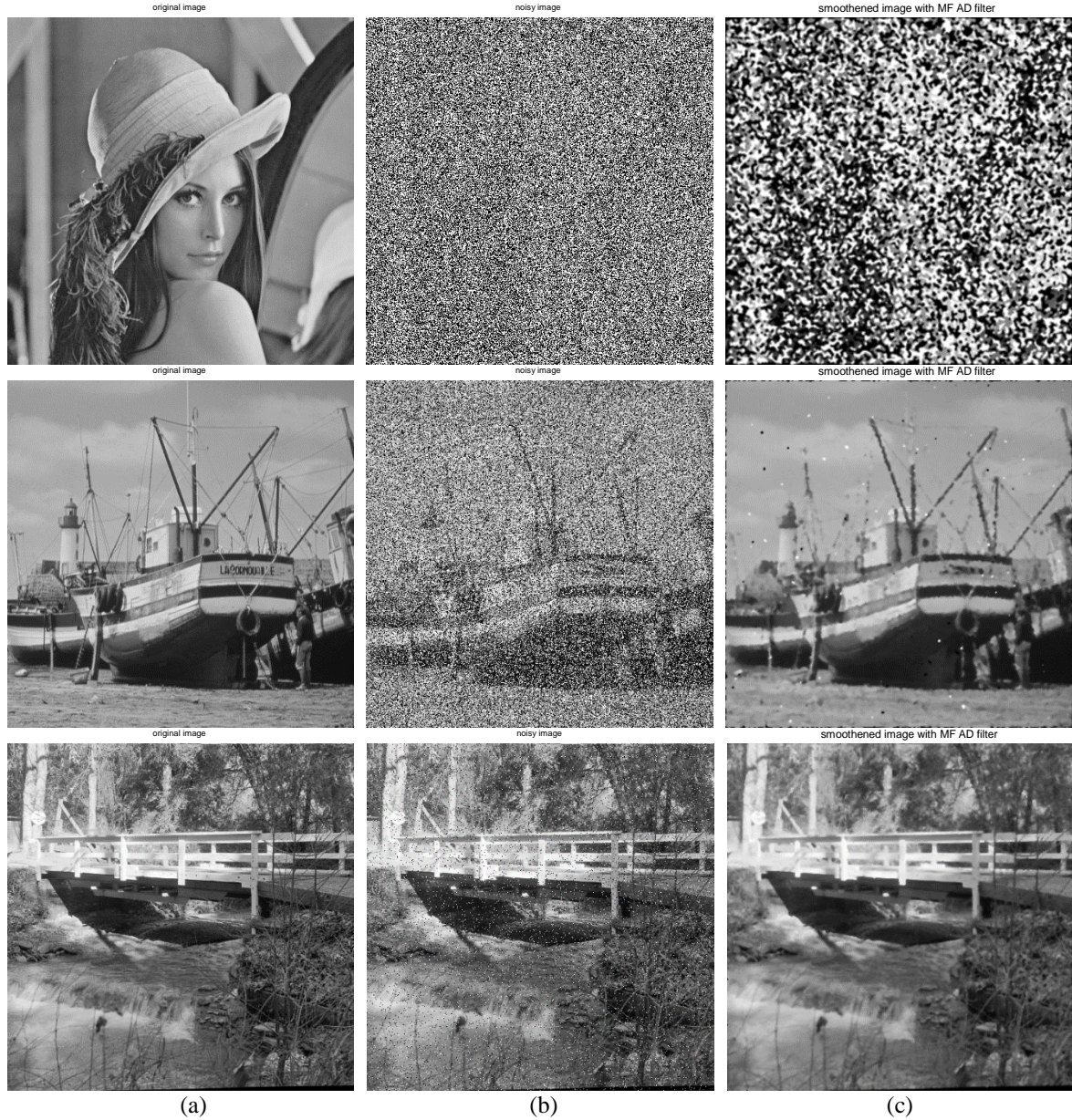


Fig. 3 (a) Original Lena (first row), Boat (second row) and Bridge images (third row) (b) corrupted by 90% (first row), 50% (second row) and 5% (third row) salt and pepper FVIN (c) filtered with MF-AD

Measures	Lena (90% FVIN)	Boat (50% FVIN)	Bridge (5% FVIN)
PSNR (dB)	9.5133	24.3647	25.4816
MAE	67.0099	7.6779	9.0813
MSE	7.2736e+003	238.0204	184.0437
MSSIM	0.04981	0.75954	0.72310

Table 1. Image quality metrics for processing corrupted Lena, Boat and Bridge images with median boosted Anisotropic Diffusion filter

Finally, a combined ST MDF-based Total Variation Regularized (TVR-ST MDF) variant was implemented to compare with the AD-based approaches. The results in Fig. 4 show that the TVR-

STMDF yields the worst results at high noise densities in addition to a large number of iterations and further increased computational complexity. Thus, this scheme was abandoned and the STMDF-AD was selected due to its consistency of quality results and relative speed, requiring fewer iterations.



Fig. 4 Filtered Lena image (corrupted with 90% salt and pepper FVIN) using (a) NAFSMF-AD and (b) STMDF-AD (c) TVR-STMDF

Measures	TVR-STMDF	MF-AD	NAFSMF-AD	STMDF-AD
PSNR (dB)	5.5771	9.5133	26.2880	27.3223
MAE	116.6913	67.0099	6.6488	6.0540
MSE	1.8004e+04	7.2736e+003	152.8552	120.4627
MSSIM	0.00856	0.04981	0.76621	0.79663

Table 2. Quantitative metrics for Filtered Lena image (corrupted with 90% salt and pepper FVIN) using MF-AD, NAFSMF-AD and STMDF-AD

3.1 Filter performance comparisons

Fig. 3 to 4 and Table 1 to 2 show that the STMDF-AD formulation yields much better results than the other AD combinations. This section compares the results of the STMDF-AD with the various filters from the literature. The images tested include the Lena, Peppers, etc. Based on the results in Table 3 and Fig. 5 show that the STMDF-AD consistently outperforms several of the known median filter variants. Additionally, the filters designed for high density noise such as NAFSMF or MDBUTMF were compared. The aspects of the filters that would normally blur edges have been mitigated. The general trend is that the STMDF dominates at high noise densities and low noise density in most cases. However, since impulse noise is highly non-linear and non-additive, the results are still quite surprising.

Filter	Lena @ 10%	Lena @ 20%	Lena @ 30%	Lena @ 40%	Lena @ 50%	Lena @ 60%	Lena @ 70%	Lena @80%	Lena @90%
Med	33.1027	28.5209	23.5908	18.804	15.1522	12.3633	9.9962	8.1546	6.6478
AMF	37.9556	34.8321	32.7849	30.4298	28.3124	26.4811	24.4653	20.3704	13.7031
MDBUTMF	37.7178	34.604	32.6131	31.3683	30.0338	29.0234	28.1496	27.137	25.3418
FIRE2n	31.86	24.6061	19.7341	15.9973	13.1915	11.0473	9.205	7.7223	6.4728
FIRE2r	34.2373	29.9134	26.4244	22.7039	19.0685	15.8659	12.7197	9.8621	7.3686
STMDF_AD	40.6408	37.4805	35.4109	34.1019	33.9	32.1	30.7609	29.41	27.4923
FESTM	34.5911	32.7889	31.1052	29.3935	27.0312	23.3868	18.7982	14.0849	9.6617
SMF	31.0467	23.2544	17.4936	13.9458	11.6021	9.818	8.2855	7.1331	6.2116
PSMF	37.0489	32.1836	29.0489	24.9683	20.6717	12.2828	9.9384	8.1176	6.6318
NAFSM	38.816	35.6916	33.6541	32.3401	30.8753	29.7736	28.6372	27.1376	23.4373
DWFM	33.6526	29.3519	23.832	18.9049	15.1278	12.3176	9.9253	8.0942	6.6083

(a)

Filter	Peppers @10%	Peppers @20%	Peppers @30%	Peppers @40%	Peppers @50%	Peppers @60%	Peppers @70%	Peppers @80%	Peppers @90%
Med	31.6302	28.1805	23.098	18.7499	15.0541	12.1611	9.8015	7.9568	6.4647
AMF	34.9864	33.6469	31.6547	29.8014	28.0815	26.3943	24.2688	20.2563	3.6766
MDBUTMF	38.5032	35.3375	33.5738	32.106	30.8644	29.7692	28.6105	27.2986	25.5261
FIRE2n	31.5853	24.389	19.4439	15.9145	13.0497	10.8476	9.0129	7.5625	6.2995
FIRE2r	34.0725	29.8773	26.3134	22.6046	19.0393	15.6859	12.5549	9.7325	7.2237
STMDF-AD	39.1913	36.4405	34.6947	33.2775	32.1014	31.1756	30.1650	29.3339	27.5463
FESTM	33.3291	31.8693	30.5704	29.0457	26.833	23.6212	19.0386	14.2936	9.9883
SMF	31.4874	21.6549	17.3826	14.5223	12.0192	10.1006	8.4668	7.1712	6.11
PSMF	36.2691	31.4148	28.0333	24.438	15.0137	12.1237	9.7637	7.9323	6.4534
NAFSM	39.519	36.3048	34.4985	32.9166	31.6165	30.4287	28.9183	27.2275	23.669
DWFM	32.1974	28.949	23.4036	18.8778	15.0752	12.1434	9.7637	7.9189	6.4568

(b)

Filter	Gold Hill @10%	Gold Hill @20%	Gold Hill @30%	Gold Hill @40%	Gold Hill @50%	Gold Hill @60%	Gold Hill @70%	Gold Hill @80%	Gold Hill @90%
Med	30.3738	27.5088	22.9758	18.6167	15.0163	12.1487	9.9252	8.032	6.5549
AMF	34.7316	33.1146	30.7087	28.7857	27.1514	25.7042	23.828	19.969	13.7588
MDBUTMF	36.2434	33.0963	31.2686	29.9325	28.9211	27.971	27.1175	26.1592	24.8885
FIRE2n	31.0727	24.472	19.5385	15.9344	13.0972	10.8758	9.1292	7.6289	6.3973
FIRE2r	33.4551	29.6473	25.9814	22.2676	18.9262	15.6088	12.6672	9.7692	7.3897
STMDF-AD	37.1380	34.5137	32.4310	31.3515	30.3708	29.5245	28.5399	27.8406	26.4769
FESTM	31.8025	30.5854	29.4478	28.0615	26.2639	23.3441	19.2596	14.7352	10.3501
SMF	31.0092	22.5898	17.3721	13.9506	11.5167	9.6903	8.313	7.1101	6.1546
PSMF	33.9631	30.8805	27.4432	24.4398	20.5103	16.2378	9.8873	8.0059	6.5421
NAFSM	37.1957	33.9979	32.1461	30.7413	29.6955	28.6354	27.6159	26.3618	23.1123
DWFM	30.8608	28.133	23.3321	18.701	15.0454	12.1284	9.885	8.0038	6.5577

(c)

Filter	Boat @10%	Boat @20%	Boat @30%	Boat @40%	Boat @50%	Boat @60%	Boat @70%	Boat @80%	Boat @90%
Med	30.4152	26.9764	22.551	18.5473	15.0613	12.2387	9.8783	8.0182	6.5112
AMF	35.1825	32.5336	30.2059	28.3305	26.6616	24.8546	23.0974	19.4761	13.5018
MDBUTMF	34.3858	31.4113	29.3917	28.1948	27.1762	26.1744	25.2691	24.3889	23.0614
FIRE2n	30.7574	24.0902	19.3184	15.9015	13.1291	10.9506	9.0938	7.5984	6.3524
FIRE2r	32.9701	28.9356	25.3348	22.0402	18.73	15.6301	12.5034	9.6918	7.2486
STMDF-AD	35.9495	33.7142	32.2112	31.0295	30.0703	28.8984	27.7683	26.5792	24.9939
FESTM	32.3517	30.9514	29.5103	28.118	25.9633	22.3425	17.9261	13.2242	8.8629
SMF	31.4778	20.9695	17.0984	14.4257	12.1527	10.2746	8.5931	7.2238	6.1552
PSMF	33.1835	29.7946	26.7411	23.7352	20.3037	16.2349	9.8519	8.0013	6.5022
NAFSM	35.7769	32.8192	30.6852	29.4707	28.3268	27.2085	26.0275	24.7979	22.1008
DWFM	30.925	27.6035	22.8411	18.6702	15.0553	12.2028	9.8102	7.9426	6.4476

(d)

Filter	Bridge @ 10%	Bridge @ 20%	Bridge @ 30%	Bridge @ 40%	Bridge @ 50%	Bridge @ 60%	Bridge @ 70%	Bridge @80%	Bridge @90%
Med	25.9369	24.2888	21.2312	17.6424	14.6564	11.9146	9.7484	7.8996	6.4669
AMF	28.6338	27.0595	25.4723	24.0825	22.8558	21.6548	20.2167	17.7652	12.8858
MDBUTMF	29.9867	27.7344	26.1779	24.9423	24.056	23.2189	22.39	21.5142	20.3954
FIRE2n	28.4151	23.1803	18.808	15.385	12.8311	10.6818	8.9627	7.4797	6.2871
FIRE2r	29.6863	26.5333	23.6657	20.5991	17.8651	14.8851	12.1551	9.4751	7.1808
STMDF-AD	30.6392	28.4242	26.8421	26.2742	24.8058	24.1869	23.3125	22.6996	21.7225
FESTM	26.9034	26.1525	25.2555	24.3432	23.1328	21.203	17.9265	14.0184	9.9545
SMF	28.1935	21.2808	16.8921	13.9209	11.6066	9.7546	8.3674	7.067	6.0993
PSMF	28.8009	26.9044	24.7095	22.0798	19.2219	11.8825	9.7073	7.8749	6.4523
NAFSM	31.3195	28.5972	26.8164	25.5224	24.4558	23.5474	22.5367	21.46	19.4492
DWFM	26.1689	24.5403	21.3825	17.632	14.6405	11.8692	9.6938	7.8534	6.4496

(e)

Filter	Jetplane @ 10%	Jetplane @ 20%	Jetplane @ 30%	Jetplane @ 40%	Jetplane @ 50%	Jetplane @ 60%	Jetplane @ 70%	Jetplane @ 80%	Jetplane @ 90%
Med	34.1955	28.8073	23.3249	18.816	15.1839	12.1237	9.8855	8.0256	6.5277
AMF	39.2939	36.4385	33.9087	31.4531	29.4069	27.4818	25.6558	20.7555	13.8314
MDBUTMF	40.7622	38.5755	36.6247	34.7777	33.7884	32.7628	31.6871	30.5502	29.088
FIRE2n	31.4109	24.601	19.735	16.0518	13.2519	10.8654	9.1243	7.6342	6.3692
FIRE2r	34.3811	30.5359	26.7771	23.1676	19.4401	15.8516	12.7486	9.8983	7.3458
STMDF-AD	42.2972	39.9119	37.9374	36.7430	35.6003	34.5760	33.2587	32.1504	30.6120
FESTM	36.9321	35.054	33.0193	30.9321	27.3182	21.9406	16.7973	11.7913	7.2401
SMF	30.9657	20.4141	17.7816	15.4367	13.1405	10.9765	9.2158	7.6662	6.3757
PSMF	37.7866	32.3406	28.2301	18.8287	15.1796	12.1159	9.8653	8.0154	6.5168
NAFSM	42.2716	39.8171	37.7997	36.0113	34.7217	33.3641	32.0672	30.2168	25.3816
DWFM	35.5726	30.3369	24.0061	19.0915	15.2346	12.0983	9.7892	7.902	6.3826

(f)

Filter	Tank @10%	Tank @20%	Tank @30%	Tank @40%	Tank @50%	Tank @60%	Tank @70%	Tank @80%	Tank @90%
Med	30.0025	27.1871	23.1893	19.024	15.4205	12.5014	10.2183	8.3542	6.8505
AMF	34.1082	32.6832	30.8218	29.146	27.8142	25.9753	24.351	20.4458	13.9375
MDBUTMF	36.2048	33.0564	31.2977	30.0399	28.9961	28.1565	27.3451	26.5535	25.4226
FIRE2n	31.4894	24.441	19.8387	16.3195	13.5142	11.2442	9.4572	7.9443	6.7124
FIRE2r	33.6	29.5137	26.1526	22.8277	19.2651	15.8706	12.9073	10.0194	7.5928
STMDF-AD	38.2077	35.3229	33.4854	31.6116	30.6974	29.5158	28.4204	27.2103	26.5622
FESTM	31.6216	30.5682	29.5289	28.3502	26.4515	23.2304	18.7967	14.1962	9.7877
SMF	34.6265	22.014	16.7271	13.8737	11.5653	9.6675	8.2693	7.1148	6.2984
PSMF	34.929	31.3565	28.5318	25.0161	21.1666	12.5204	10.2166	8.3477	6.8458
NAFSM	36.8193	33.6768	31.9032	30.6355	29.5314	28.6312	27.6246	26.4707	23.6473
DWFM	30.3836	27.741	23.4497	19.1523	15.4202	12.4701	10.1648	8.2971	6.8156

(g)

Filter	Elaine @10%	Elaine @20%	Elaine @30%	Elaine @40%	Elaine @50%	Elaine @60%	Elaine @70%	Elaine @80%	Elaine @90%
Med	31.3272	28.3503	23.4363	18.909	15.4152	12.2336	10.0335	8.139	6.6519
AMF	35.5045	34.253	32.2521	30.1324	28.5876	26.8843	24.9864	20.5869	13.9379
MDBUTMF	39.9138	36.7861	34.9578	33.4897	32.4413	31.2611	30.2057	28.9556	27.1654
FIRE2n	31.937	24.7876	19.6886	16.151	13.3754	10.9735	9.2395	7.7395	6.4954
FIRE2r	34.2477	30.3112	26.7043	22.9129	19.4948	15.8724	12.8454	9.8421	7.4121
STMDF-AD	40.2527	37.5168	35.7253	34.4048	33.1160	31.7822	30.9592	30.0927	28.5875
FESTM	33.2129	32.0517	30.7888	29.4232	27.1043	23.036	18.239	13.3867	9.0827
SMF	31.8305	22.8719	17.4789	13.9509	11.493	9.6382	8.2987	7.1368	6.2142
PSMF	36.4616	32.3524	28.7944	25.0043	21.0951	16.4339	10.009	8.1197	6.6415
NAFSM	40.7298	37.5434	35.6673	34.1886	32.9855	31.6996	30.4155	28.8028	24.5467
DWFM	32.1092	29.1776	23.8458	19.0844	15.4385	12.1877	9.9636	8.0631	6.5831

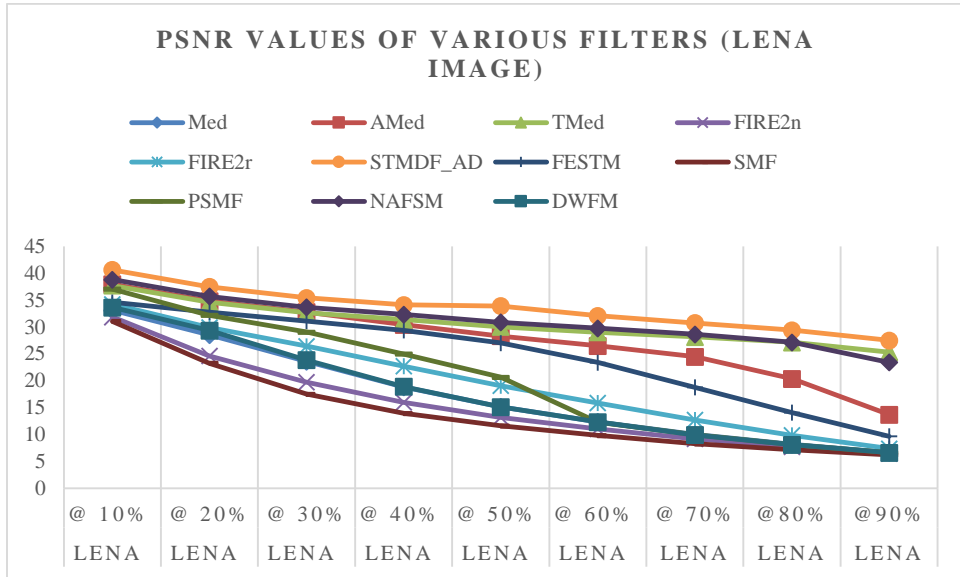
(h)

Filter	Truck @10%	Truck @20%	Truck @30%	Truck @40%	Truck @50%	Truck @60%	Truck @70%	Truck @80%	Truck @90%
Med	32.1546	28.8389	23.8224	19.2901	15.5132	12.6205	10.2793	8.4576	6.9474
AMF	36.3487	34.6487	32.7765	30.9503	29.1538	27.3257	25.2459	20.9441	14.3348
MDBUTMF	37.7222	34.7338	32.8943	31.5181	30.5048	29.6064	28.7801	27.9462	26.7139
FIRE2n	31.9867	24.8464	20.0254	16.3969	13.524	11.3183	9.4936	8.039	6.7778
FIRE2r	34.4967	30.4041	26.8902	23.2645	19.413	16.1164	13.0723	10.1948	7.7374
STMDF-AD	40.8972	37.6033	35.4602	33.2920	33.1305	31.9333	30.6792	29.3114	28.2050
FESTM	33.8763	32.4549	31.0904	29.6947	27.7566	24.5713	20.1599	15.6916	11.2521
SMF	35.0657	24.8048	18.594	13.1164	10.5324	9.0084	7.9454	7.0979	6.3562
PSMF	36.9988	33.3732	29.9112	26.1816	21.4643	12.6218	10.2706	8.4476	6.9416
NAFSM	38.6716	35.6235	33.8183	32.3636	31.3197	30.3379	29.3057	27.9503	24.6171
DWFM	32.5286	29.2279	23.9675	19.3083	15.4854	12.5822	10.2358	8.4287	6.9528

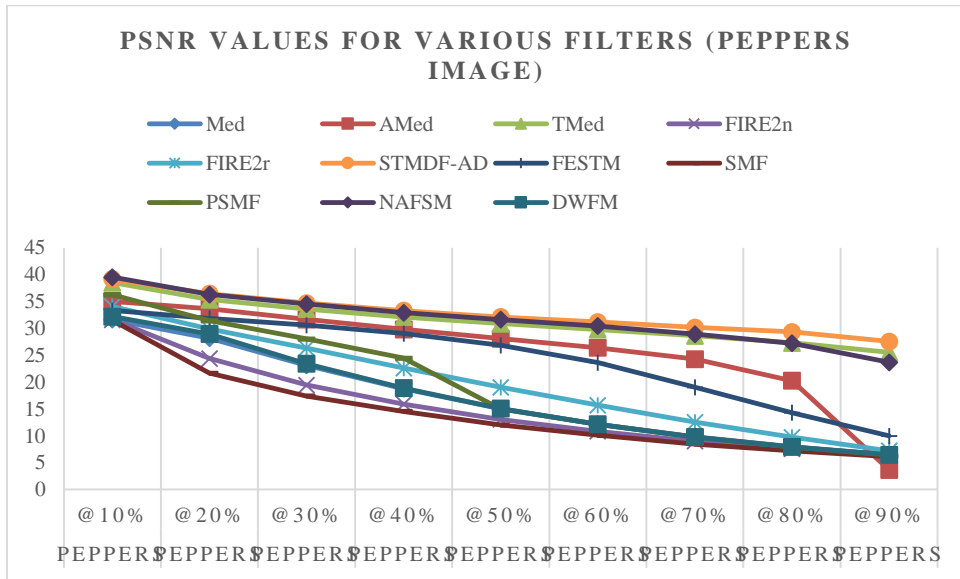
(i)

Table 3. PSNR values for the filtered (a) Lena (b) Peppers (c) Gold Hill (d) Boat (e) Bridge (f) Jetplane (g) Tank (h)

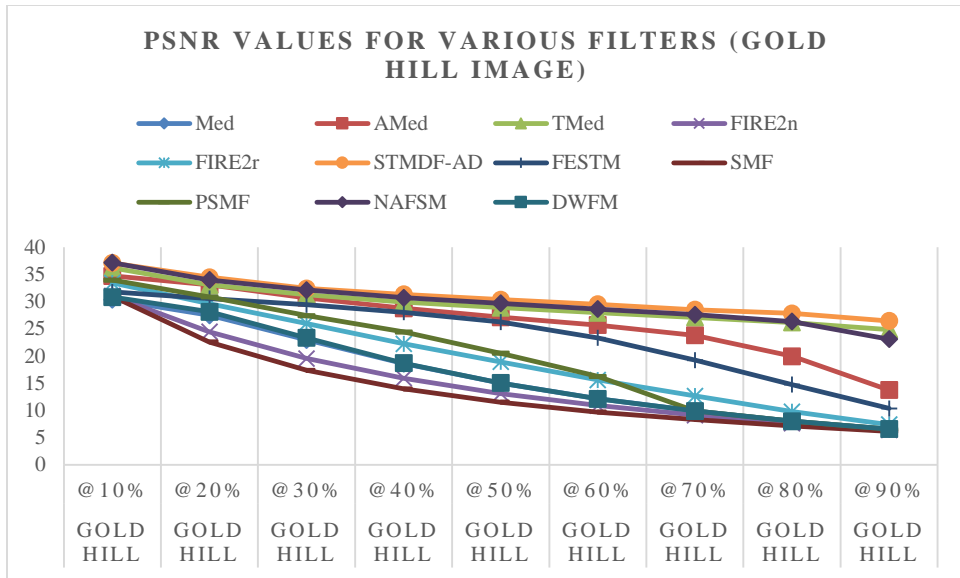
Elaine (i) Truck image corrupted by varying levels of FVIN noise



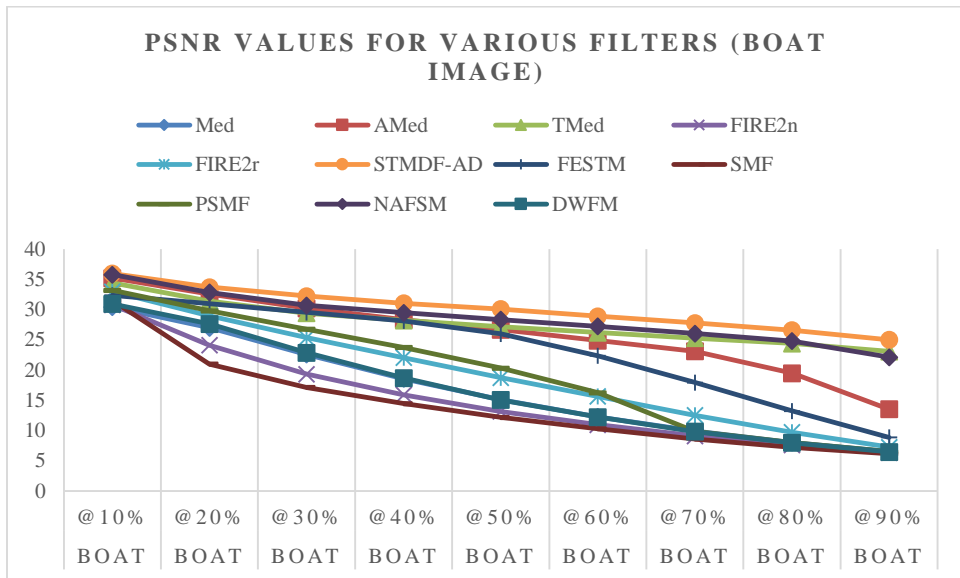
(a)



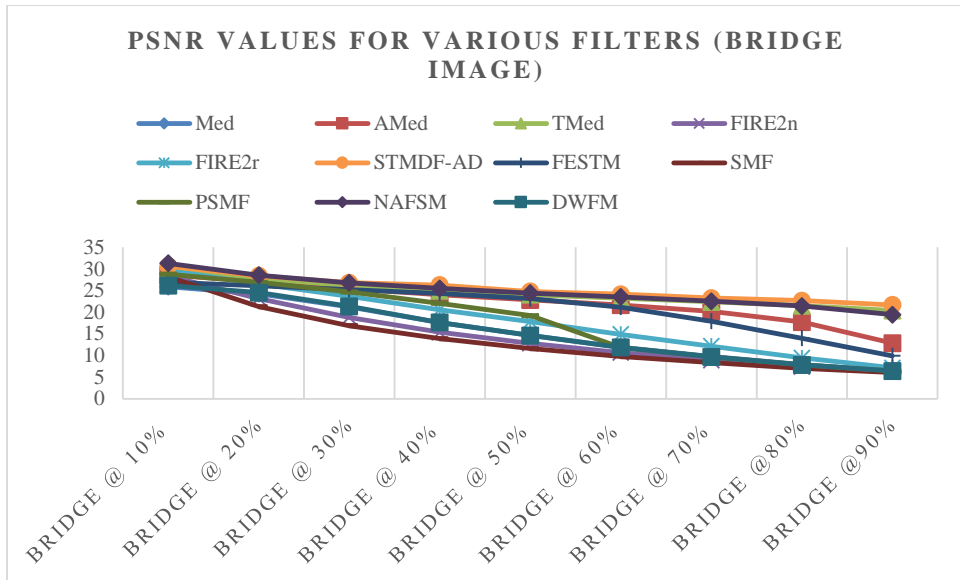
(b)



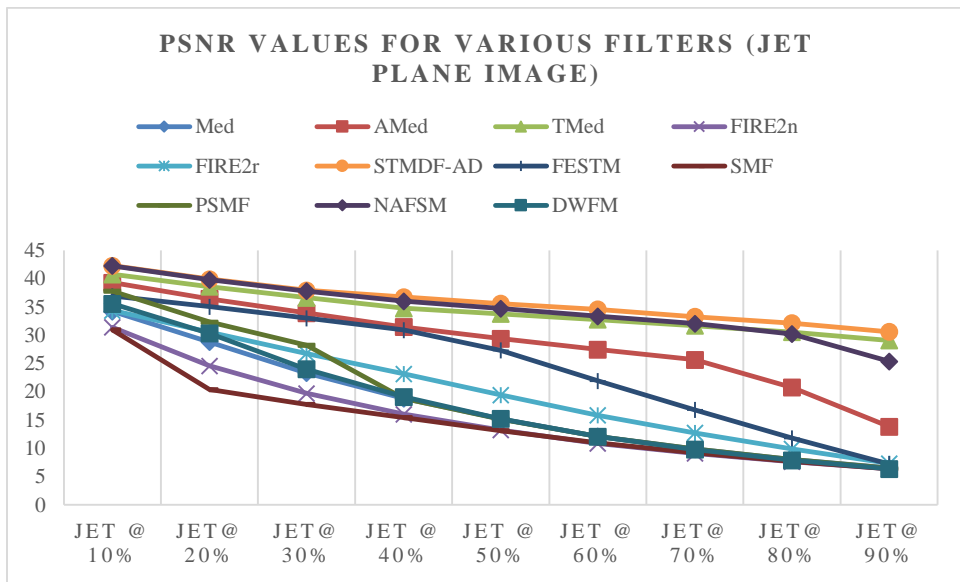
(c)



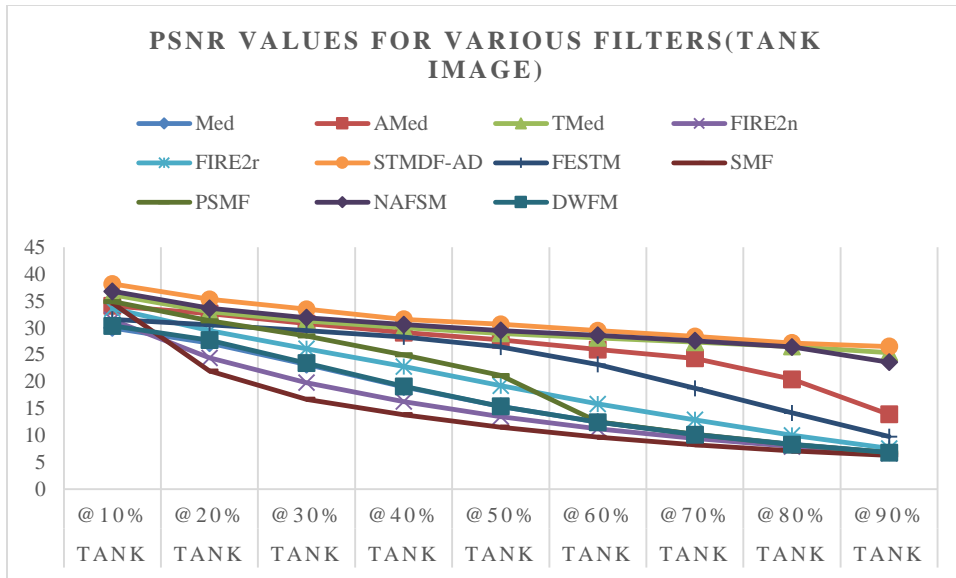
(d)



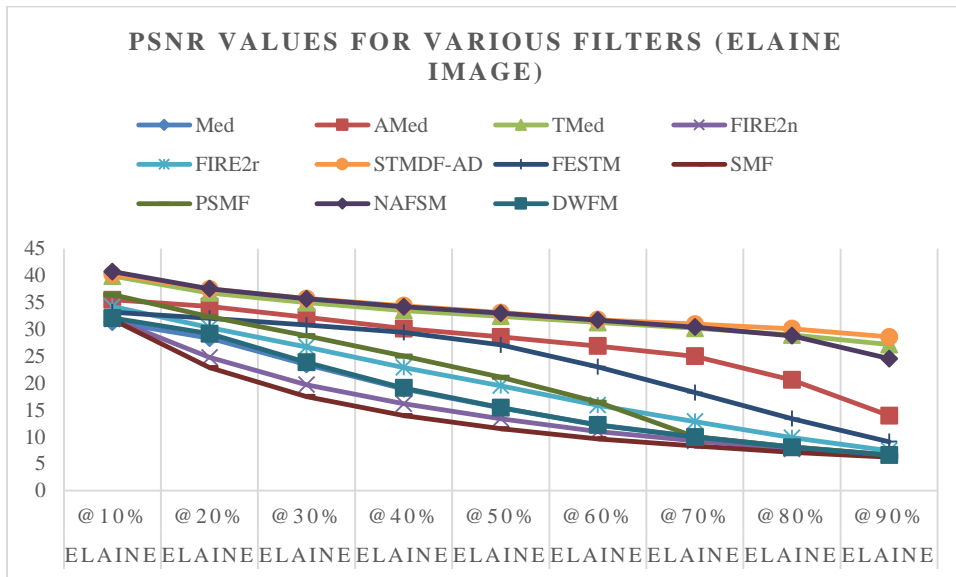
(e)



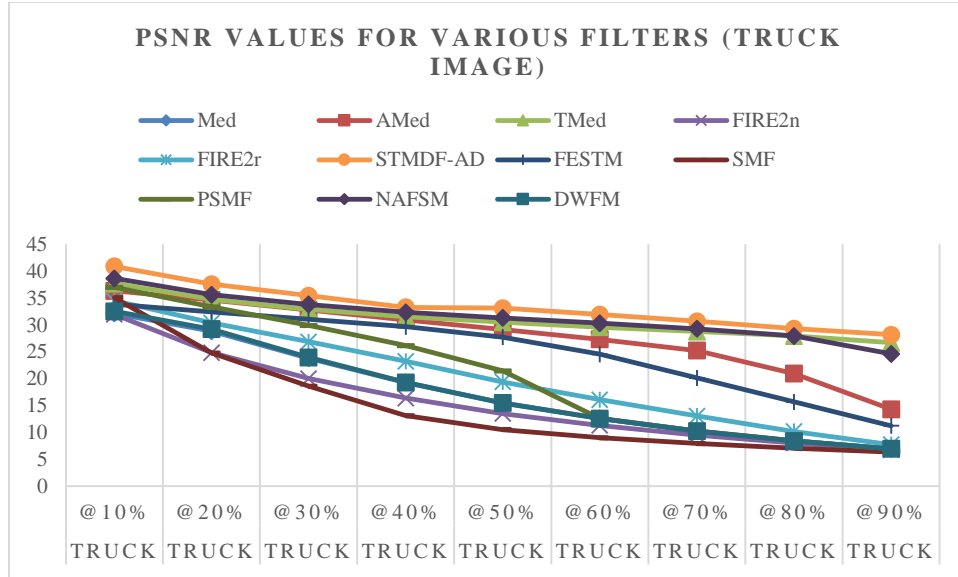
(f)



(g)



(h)



(i)

Fig. 5. PSNR values for the filtered (a) Lena (b) Peppers (c) Gold Hill (d) Boat (e) Bridge (f) Jetplane (g) Tank (h) Elaine (i) Truck image corrupted by varying levels of FVIN noise

The results in Table 5 once more indicates the complete domination of the proposed algorithm at even high noise densities (95%) over the other compared filters, especially the ones suited to high density noise.

Filter	Lena @ 10%	Lena @ 20%	Lena @ 30%	Lena @ 40%	Lena @ 50%	Lena @ 60%	Lena @ 70%	Lena @ 80%	Lena @ 90%
Med	2.8125	3.5894	5.3008	9.4641	17.3464	29.5304	47.6341	70.6258	97.9845
AMF	0.9699	1.3111	1.812	2.465	3.3512	4.3998	5.841	9.2384	24.5079
MDBUTMF	0.5651	1.1505	1.7702	2.3665	3.064	3.777	4.5245	5.4327	7.0298
FIRE2n	1.5068	3.9108	8.258	15.6119	26.3763	40.2507	58.2288	79.2356	102.8278
FIRE2r	1.3681	2.8402	4.7136	7.4604	12.0432	19.4367	32.4942	54.4271	87.5895
STMDf-AD	0.4248	0.8768	1.3686	1.8617	2.4783	2.6302	3.8897	4.7378	5.9844
FESTM	2.5696	3.1186	3.8006	4.5864	5.6868	7.6027	12.1309	23.9798	54.1608
SMF	1.1527	4.4487	12.5529	24.2584	37.9379	53.6621	72.1496	90.7215	109.1785
PSMF	0.5843	1.2157	2.0827	3.7136	7.3531	29.8466	48.4943	71.6735	98.7092
NAFSM	0.5037	1.0231	1.5868	2.132	2.792	3.4579	4.2123	5.2067	7.5689
DWFM	2.7743	3.4679	5.1802	9.3155	17.3878	29.7703	48.3054	71.5431	98.853

(a)

Filter	Peppers @10%	Peppers @20%	Peppers @30%	Peppers @40%	Peppers @50%	Peppers @60%	Peppers @70%	Peppers @80%	Peppers @90%
Med	3.3749	4.0596	5.788	9.6379	17.4401	29.9491	48.0263	71.1551	98.4177
AMF	1.7333	1.8577	2.2217	2.7951	3.5939	4.5503	5.9577	9.2714	24.1218
MDBUTMF	0.5346	1.0887	1.6384	2.2398	2.8539	3.5416	4.2944	5.2707	6.7938
FIRE2n	1.5046	3.9571	8.3228	15.3432	26.2129	40.499	58.4639	9.1549	102.9972
FIRE2r	1.358	2.8471	4.6705	7.3413	11.8066	19.4558	32.4752	4.1012	87.299
STMDF-AD	0.5695	1.1342	1.6975	2.6276	3.4453	3.8265	4.8752	5.1978	6.3560
FESTM	3.0628	3.6136	4.2184	4.9803	6.0304	7.7686	12.1054	23.4441	51.0838
SMF	1.0818	5.9605	12.9354	21.903	34.6948	49.688	67.8128	87.6864	107.947
PSMF	0.6466	1.4474	2.5005	4.1881	16.5319	29.6266	48.3915	71.7782	98.9256
NAFSM	0.4959	1.0051	1.5075	2.0725	2.6564	3.308	4.0835	5.1419	7.3529
DWFM	3.3222	3.9444	5.6405	9.4811	17.3982	30.0925	48.4829	71.8637	98.8587

(b)

Filter	Gold Hill @10%	Gold Hill @20%	Gold Hill @30%	Gold Hill @40%	Gold Hill @50%	Gold Hill @60%	Gold Hill @70%	Gold Hill @80%	Gold Hill @90%
Med	4.2472	5.0012	6.8065	10.8842	18.6689	31.1852	48.5912	71.7952	98.49
AMF	1.4532	1.8598	2.5104	3.3342	4.3494	5.5558	7.1987	10.8972	25.2825
MDBUTMF	0.7968	1.6145	2.4436	3.2965	4.1604	5.0735	6.0207	7.1712	8.7866
FIRE2n	1.6601	4.1262	8.5914	15.8461	26.6661	41.0512	58.5167	79.4677	102.7248
FIRE2r	1.5028	3.0435	5.0134	7.9659	12.4717	20.2472	33.0117	54.9444	86.3491
STMDF-AD	0.7052	1.3712	2.2790	3.0387	3.8744	4.6311	5.6119	6.6332	7.8370
FESTM	3.8372	4.4313	5.103	5.9407	6.9998	8.7623	12.8027	23.3685	50.187
SMF	1.2888	5.1993	12.9434	24.2575	38.3142	54.235	71.0251	89.8036	108.67
PSMF	1.0222	1.8142	2.9847	4.6623	8.0148	15.5688	48.8637	72.4581	99.0538
NAFSM	0.7169	1.4545	2.2081	2.994	3.7956	4.6741	5.6072	6.8224	9.272
DWFM	4.1995	4.9017	6.648	10.7712	18.6121	31.3672	49.0533	72.3927	98.7938

(c)

Filter	Boat @10%	Boat @20%	Boat @30%	Boat @40%	Boat @50%	Boat @60%	Boat @70%	Boat @80%	Boat @90%
Med	3.7314	4.6318	6.5804	10.5839	18.129	30.4602	48.5204	71.3438	98.4811
AMF	1.2673	1.7122	2.3814	3.1892	4.216	5.5024	7.196	10.9693	25.7975
MDBUTMF	0.8146	1.6338	2.5132	3.3475	4.226	5.1757	6.1681	7.3423	9.1141
FIRE2n	1.7474	4.3368	8.8813	15.9682	26.5491	40.6269	58.693	79.5176	102.9133
FIRE2r	1.5842	3.2023	5.303	8.214	12.8423	20.4607	33.8505	55.6071	87.8882
STMDF - AD	0.7491	1.3830	2.0328	2.7155	3.4055	4.3090	5.2925	6.4474	7.9950
FESTM	3.2586	3.8488	4.555	5.372	6.5084	8.6402	13.5597	26.6855	59.3964
SMF	1.1197	6.7716	13.7878	22.5186	34.0741	48.4934	66.656	87.0572	107.7068
PSMF	1.0979	1.9554	3.1801	4.9583	8.1556	15.4257	48.6142	71.702	98.8604
NAFSM	0.7114	1.4271	2.2079	2.9487	3.7661	4.6441	5.6546	6.9152	9.4466
DWFM	3.6764	4.5035	6.4194	10.4254	18.1326	30.6521	49.1487	72.3784	99.6529

(d)

Filter	Bridge @10%	Bridge @20%	Bridge @30%	Bridge @40%	Bridge @50%	Bridge @60%	Bridge @70%	Bridge @80%	Bridge @90%
Med	7.3923	8.4446	10.6144	15.1312	22.4358	34.7467	51.7067	73.9766	99.0583
AMF	2.9055	3.5607	4.6483	6.0311	7.6397	9.6918	12.353	16.9798	32.1718
MDBUTMF	1.7154	3.1709	4.6627	6.1698	7.6541	9.2071	10.8724	12.8413	15.4789
FIRE2n	2.8113	5.7018	10.6868	18.4476	28.8274	43.1165	60.3597	81.0394	103.137
FIRE2r	2.6216	4.5721	7.0929	10.6458	15.5358	23.8751	36.9649	58.4438	88.6215
STMDF-AD	1.4334	2.7127	3.9777	4.5839	7.5363	9.0036	10.6044	12.0269	14.6781
FESTM	6.5273	7.266	8.1282	9.1531	10.3587	12.362	16.7488	27.4376	53.5846
SMF	2.0075	6.6713	14.3818	24.5498	37.5339	52.9196	69.3644	88.8516	107.6434
PSMF	2.3306	3.576	5.2279	7.6675	11.4076	33.4184	51.4047	74.153	99.4896
NAFSM	1.4298	2.7888	4.2035	5.5951	7.0577	8.5622	10.2764	12.3344	15.932
DWFM	7.3074	8.3293	10.4821	15.1006	22.456	35.0012	52.2575	74.7082	99.566

(e)

Filter	Jetplane @ 10%	Jetplane @ 20%	Jetplane @ 30%	Jetplane @ 40%	Jetplane @ 50%	Jetplane @ 60%	Jetplane @ 70%	Jetplane @ 80%	Jetplane @ 90%
Med	1.6999	2.1968	3.7501	7.5088	14.9427	28.2407	46.1069	69.4648	97.3867
AMF	0.8916	0.9355	1.1214	1.4409	1.8528	2.4392	3.2013	6.0166	20.4056
MDBUTMF	0.2828	0.5408	0.8241	1.1364	1.4278	1.7335	2.0745	2.4691	3.0664
FIRE2n	1.448	3.6764	7.7893	14.7517	25.0617	40.1547	57.6106	78.4602	102.5338
FIRE2r	1.2985	2.5943	4.265	6.6798	10.845	18.5225	31.4684	52.7336	86.3684
STMDF-AD	0.2684	0.5186	0.7892	1.0605	1.3441	1.6689	2.1212	2.4849	3.1874
FESTM	1.5799	1.8817	2.3539	2.9794	4.0056	6.4185	12.3501	29.074	72.8688
SMF	0.9537	7.7057	12.8097	19.376	28.9139	42.4418	59.1248	79.6127	103.1506
PSMF	0.3274	0.7174	1.3689	6.6092	14.2706	27.8234	46.2323	69.6391	97.8809
NAFSM	0.2522	0.4906	0.7537	1.0318	1.3179	1.629	1.9705	2.4386	3.8593
DWFM	1.6596	2.0564	3.5141	7.2354	14.851	28.4103	46.9526	71.001	99.6992

(f)

Filter	Tank @10%	Tank @20%	Tank @30%	Tank @40%	Tank @50%	Tank @60%	Tank @70%	Tank @80%	Tank @90%
Med	4.9559	5.7361	7.4633	11.3951	19.049	31.6686	49.3562	72.1634	99.1763
AMF	1.7643	2.1838	2.8415	3.6791	4.7078	6.0771	7.7376	11.4357	26.5359
MDBUTMF	0.8841	1.8052	2.7083	3.6148	4.5517	5.4949	6.5231	7.6413	9.2151
FIRE2n	1.6208	4.2371	8.6382	15.7335	26.4167	40.9927	58.7311	79.8464	103.0507
FIRE2r	1.4801	3.0907	5.0658	7.8085	12.4395	20.4068	33.3828	55.6825	88.0801
STMDF-AD	0.6772	1.3648	2.0720	2.9372	3.8250	4.8844	6.0007	7.3552	8.4341
FESTM	4.329	4.8585	5.4635	6.2168	7.2345	9.0917	13.6646	25.5152	55.821
SMF	0.8392	5.5012	14.5808	25.1813	39.2437	56.6947	74.9126	94.4931	111.949
PSMF	0.9472	1.7628	2.7821	4.3859	7.3788	29.9134	48.3657	71.832	99.2161
NAFSM	0.8165	1.6703	2.5114	3.3545	4.2493	5.1518	6.1997	7.4147	9.7489
DWFM	4.8967	5.6128	7.3225	11.2253	19.0446	31.8481	49.895	73.043	99.9878

(g)

Filter	Elaine @10%	Elaine @20%	Elaine @30%	Elaine @40%	Elaine @50%	Elaine @60%	Elaine @70%	Elaine @80%	Elaine @90%
Med	4.2704	4.8658	6.5155	10.4514	17.6577	31.0104	48.3497	71.6879	98.4158
AMF	1.5714	1.86	2.3711	3.074	3.9187	5.005	6.4295	9.8205	24.213
MDBUTMF	0.5769	1.1642	1.764	2.3879	3.0112	3.7129	4.4602	5.3896	6.7497
FIRE2n	1.4688	3.838	8.2626	15.3089	25.7198	40.8155	58.2919	79.4022	102.6757
FIRE2r	1.3381	2.7735	4.6008	7.3093	11.5488	19.3666	32.1332	54.8584	86.8807
STMDF-AD	0.5638	1.1021	1.6482	2.2397	2.8903	3.6962	5.1324	5.5921	6.3919
FESTM	3.7812	4.209	4.7668	5.4173	6.3727	8.3545	13.1911	26.2434	58.2226
SMF	1.12	4.9036	12.6834	24.3911	39.0319	55.4838	72.417	91.0257	109.4336
PSMF	0.6698	1.4517	2.5065	4.1221	7.1139	14.576	48.1992	72.0024	98.8315
NAFSM	0.5386	1.0852	1.651	2.2366	2.8419	3.5257	4.2842	5.2547	7.3813
DWFM	4.2099	4.7483	6.3401	10.2372	17.5995	31.2792	48.9937	72.7459	99.6708

(h)

Filter	Truck @10%	Truck @20%	Truck @30%	Truck @40%	Truck @50%	Truck @60%	Truck @70%	Truck @80%	Truck @90%
Med	3.5255	4.1832	5.8861	9.7584	17.5708	30.0494	48.1125	70.6795	97.7899
AMF	1.2452	1.5778	2.0936	2.7588	3.5999	4.6967	6.141	9.5321	23.6759
MDBUTMF	0.6894	1.3856	2.0907	2.8195	3.5426	4.3076	5.1022	5.99	7.3113
FIRE2n	1.4907	3.9059	8.2236	15.3216	26.1699	40.3531	58.3762	78.8834	102.3647
FIRE2r	1.3504	2.7966	4.6086	7.2137	11.7628	19.2232	32.0794	53.9943	86.0291
STMDF-AD	0.4770	0.9890	1.5557	2.1634	2.6593	3.3708	4.6142	5.3278	6.5461
FESTM	3.1312	3.6248	4.2284	4.9609	5.9419	7.6539	11.6835	21.6414	47.5109
SMF	0.6969	3.2236	9.7014	27.8904	47.2536	64.4859	80.2095	95.7251	111.7216
PSMF	0.6565	1.2717	2.1413	3.4537	6.4147	28.8634	47.5109	70.5578	97.8903
NAFSM	0.6198	1.2499	1.8797	2.5543	3.2225	3.9405	4.7236	5.7003	7.7499
DWFM	3.4746	4.0975	5.7795	9.6788	17.6042	30.2573	48.5947	71.3011	98.096

(i)

Table 4. MAE values for the filtered (a) Lena (b) Peppers (c) Gold Hill (d) Boat (e) Bridge (f) Jetplane (g) Tank (h) Elaine (i) Truck image corrupted by varying levels of FVIN noise

Filter	Chip @95%	Moon @95%	Lena @95%	Boat @95%	Peppers @95%	GoldHill @95%	Bridge @95%	Barbara @95%	Jetplane @95%	Truck @95%
Med	5.2314	6.3761	6.021	5.891	5.8148	5.8934	5.7928	5.812	5.8685	6.2952
AMF	8.9291	10.382	10.1021	9.8221	9.8378	9.9121	9.4883	9.7172	9.9021	10.3407
MDBUTMF	21.1781	25.3215	23.4188	21.3852	23.181	22.8706	19.042	20.3106	25.9447	25.0701
FIRE2n	5.2628	6.3327	5.9415	5.829	5.7529	5.8265	5.7206	5.732	5.8186	6.2161
FIRE2r	5.6461	6.7374	6.3681	6.233	6.1689	6.1752	6.0619	6.1031	6.2322	6.5983
STMDF-AD	24.8560	26.2721	25.464	23.1929	25.2743	23.9935	20.4600	21.5561	28.7487	26.7376
FESTM	5.7666	7.7999	7.6282	6.7953	7.8678	8.3424	7.9873	7.8025	5.1746	9.2241
SMF	5.3125	6.0633	5.8117	5.7218	5.6509	5.706	5.6111	5.6368	5.7951	6.0175
PSMF	5.2115	6.3749	6.0137	5.8867	5.81	5.8872	5.7864	5.8033	5.8636	6.2927
NAFSM	15.4329	17.8306	17.0449	16.4001	16.6602	16.7081	15.295	15.9605	17.2913	17.4006
DWFM	5.2516	6.36	5.9988	5.8485	5.8213	5.9133	5.8072	5.8131	5.7251	6.3251

(a)

Filter	Chip @95%	Moon @95%	Lena @95%	Boat @95%	Peppers @95%	GoldHill @95%	Bridge @95%	Barbara @95%	Jetplane @95%	Truck @95%
Med	114.2798	112.7003	112.3466	112.766	113.2729	113.2921	113.6451	113.4659	112.7317	112.5882
AMF	51.241	49.6793	48.2025	50.6212	49.339	50.2664	56.4144	52.9575	46.3373	49.0485
MDBUTMF	7.7863	8.8244	8.9429	11.486	9.0745	11.0859	18.697	14.6473	4.5513	8.9322
FIRE2n	114.9241	114.506	114.8477	114.9192	115.4342	115.4344	115.6781	115.7186	115.0038	115.0504
FIRE2r	107.4686	106.2299	106.3822	107.0383	106.9891	108.2397	108.928	108.3514	106.8399	107.1618
STMDF-AD	5.6351	8.1911	7.4677	9.8832	7.9239	10.1213	16.6855	13.0784	3.7888	7.8772
FESTM	97.4034	84.0067	81.7432	90.3358	77.9901	74.6526	78.0441	79.4866	113.4079	71.2645
SMF	114.0967	120.6731	118.3374	117.6751	118.2608	118.6601	118.347	118.197	115.8823	119.8287
PSMF	115.8352	112.7209	112.7417	113.0028	113.5493	113.6463	113.901	113.879	113.0009	112.672
NAFSM	15.7147	15.1747	15.3445	17.9326	16.0467	17.5691	25.037	20.9789	11.8666	15.5563
DWFM	114.132	113.1506	112.9243	113.6319	113.398	113.2139	113.6116	113.6368	115.1898	112.4404

(b)

Table 5. (a) PSNR and (b) MAE values for the test images corrupted with 95% FVIN and filtered with the various filters (a) Lena (b) Peppers (c) Gold Hill (d) Boat (e) Bridge (f) Jetplane (g) Baboon (h) Barbara (i) Truck (j) Moon (k) Chip image corrupted by varying levels of FVIN noise

The fuzzy filters to be compared against the proposed filter include the standard median filter (Med), the recursive (FIREr) and non-recursive (FIREn) Fuzzy FIRE filters [18], Fuzzy Estimate Select Type Median Filter (FESTMF) [38] and Directional Weighted Fuzzy Median Filter (DWFMF) [39]. Based on experiments, most of the Fuzzy filters break down around the 30% to 50% noise density region. The STMDF-AD and NAFSMF algorithms yield the best qualitative results, which correspond to the two consistently highest PSNR values in Table 5.

The results from Table 5 show that the performance of the NAFSMF drops off relatively faster than that of the STMDF-AD with increasing noise density, especially around the 80% to 90% mark. This is due to the cautious nature of the STMDF-AD, which is incremental in its filtering (in addition to the entropy guided threshold) to withstand the degrading effects of the high noise

levels. Comparing the visual results from Fig. 6 at impulse noise density of 90%, only the AMF, MDBUTMF (TMF), STMDf-AD, NAFSMF successfully filtered the noise. This is to be expected since the majority of these algorithms incorporate the switching scheme-based impulse noise detection methods in addition to iterative operation. The Switching MF and the PSMF also utilize switching but are only effective at relatively low noise levels. The Fuzzy and AMF filters are most effective at low to medium to moderately increased noise levels.

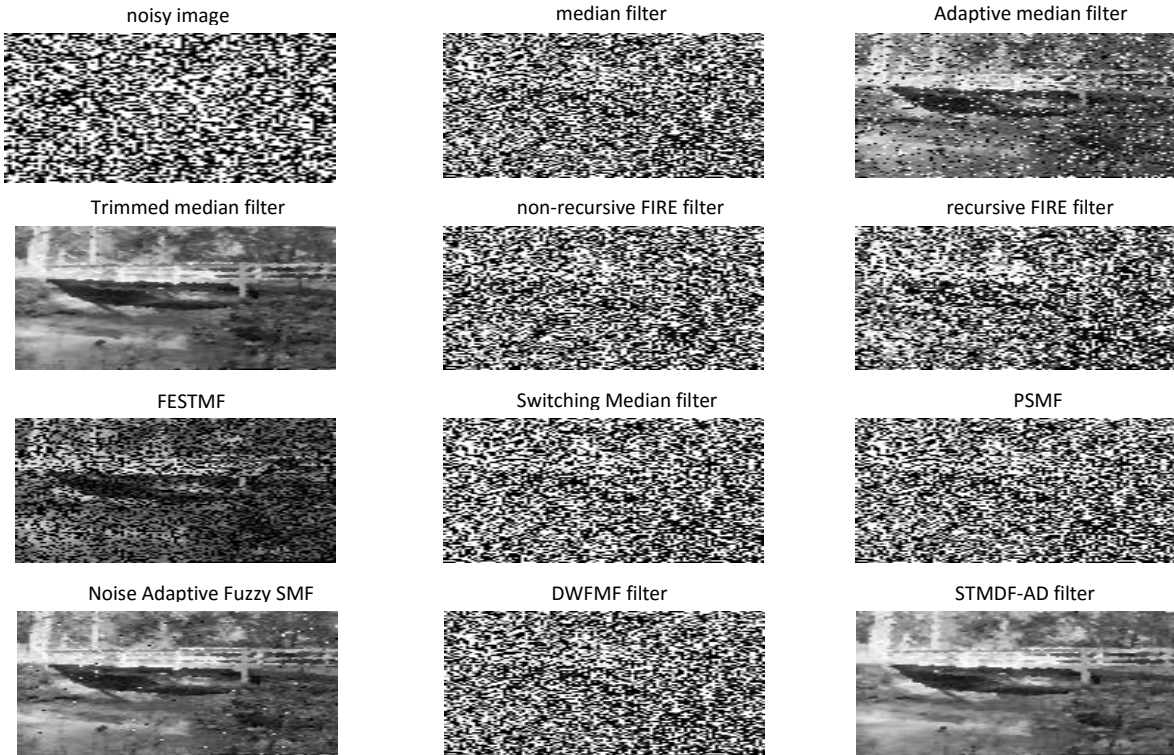


Fig. 6 Visual performance for filters denoising Bridge image corrupted with salt and pepper impulse noise (density=90%) for the various non-Fuzzy and Fuzzy Median Filters compared with the STMDf

In summary, the MDBUTMF, NAFSMF, STMDf-AD, AMF, PSMF and Fuzzy FIRE filters dominate at medium noise density levels. At high noise levels, mostly only the MDBUTMF, STMDf-AD and NAFSMF dominate. The AMF appears to be the least robust of the adaptive and iterative filters and the STMDf-AD is the highest performing filter at very high noise density levels.

3.2 Comparisons with other contemporary high density noise filters

In Fig. 7, we show a sample of images corrupted with 90% salt and pepper impulse noise processed with the STMDf-AD filter. Visually, it can be seen that the filter recovers most of the original signal amidst such high level of noise even when the image signal is indiscernible to the human eye.

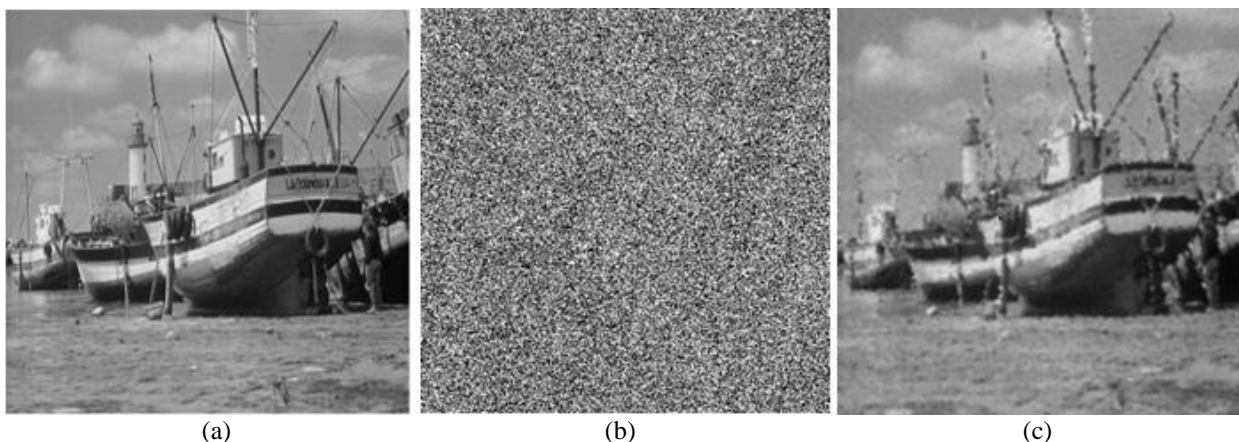


Fig. 7 (a) Original Boat image (b) image corrupted with salt and pepper noise (ND = 90%) (c) filtered image using ST MDF-AD

The other relatively recent high density noise filters from the literature compared with proposed algorithm include the Decision-Based Algorithm (DBA), the Median Filters with Regularization Chan, et al, the Fuzzy Cellular Automata (FCA) algorithm, Iterated Truncated Mean Filter (ITMF), DDBSM, ISM, SAWM, Edge Preserving Algorithm (EPA), Open and Close Filter (OCS), Linear Predictive Coding Switching Median Filter (LPC-SMF), DAM, CM and FEMF in addition to NASSM and NAFSMF and MDBUTMF. The results are presented in Table 6 to 8 and Figs 8 to 11. Based on the visual and quantitative results, the ST MDF-AD once more dominates at high to extreme noise density levels of salt and pepper impulse noise.

Table 6 Comparison of Lena and Bridge images filtered with various filters from [38] and ST MDF-AD

Algorithm	PSNR	PSNR	PSNR	SSIM	SSIM	PSNR	PSNR	PSNR
	(Lena)	(Lena)	(Lena)	(Bridge)	(Lena)	(Bridge)	(Bridge)	(Bridge)
	ND	ND	ND	ND	ND	ND	ND	ND
	(50%)	(60%)	(70%)	(70%)	(70%)	(50%)	(60%)	(70%)
PSM	24.7	24.4	19.4	0.7	0.55	22.2	19.8	17
DDBSM	24.5	21.8	17.4	0.32	0.27	22.4	19.2	15.9
ISM	27.7	24.9	23.3	0.68	0.45	23.1	22.7	20.1
NASM	28.9	24.6	21.7	0.7	0.52	24.5	22.8	19.9
Srinivasan & Ebenezer	32.2	30.4	28.6	0.84	0.74	26.1	24.2	23.1
Ching, et al	32.6	31.2	29.7	0.74	-	-	-	-
Chan, et al	31.8	30.8	29.7	0.86	0.755	28.1	26.7	25
Fuzzy Cellular Automata	31.8	30.5	29.2	0.88	0.757	26.5	25.3	24.1
ITMF	30.6	29.7	28.5	0.86	0.9422	23.7	22.9	21.9
ST MDF-AD	32.7	31.3	30.8	0.87	0.9466	24.8	24.4	23.7

Table 7 PSNR comparison of Lena images filtered with various filters from [38] and ST MDF-AD

Algorithm	ND (50%)	ND (60%)	ND (70%)	ND (80%)	ND (90%)
Srinivasan & Ebenezer	26.8	26.1	25.5	24.49	N/A
Chan, et al	27.3	26.1	24.1	22.39	25.4
Wang, et al	28.5	27.3	26	24.53	N/A
Fuzzy Cellular Automata	28.7	27.6	26.1	24.68	N/A
ITMF	30.6	29.7	28.5	27.40	25.11
PA (ST MDF-AD)	32.7	31.3	30.8	29.41	27.42

Table 8 PSNR comparison of the top performing filters from the literature against the STMDF-AD

ND (%)	Chan, et al [17]	LPC- SMF [40]	OCS [41]	EPA [42]	SAWM [43]	DAM [44]	CM [45]	FEMF [46]	ITMF [47]	(STMDF-AD)
50	N/A	31.393 (Boat)	30.63(Lena)	34.10(Lena)	33.82(Lena)	32.78(Lena)	33.85(Lena)	33.28(Lena)	30.6348 (Lena)	30.3454 (Boat) 32.7293 (Lena) 24.8058 (Bridge)
60	N/A	N/A	30.55(Lena)	32.66(Lena)	32.32 (Lena)	31.24(Lena)	32.11(Lena)	31.64(Lena)	29.7 (Lena)	31.3494 (Lena)
70	29.3 (Lena), 25.0 (Bridge)	28.133 (Lena), 26.775 (Boat)	29.71(Lena)	31.03(Lena)	30.69 (Lena)	29.68(Lena)	30.71(Lena)	30.18(Lena)	28.5 (Lena)	30.7609 (Lena) 27.2360 (Boat) 24.0122 (Bridge)
80	N/A	25.836 (Lena) 24.555 (Boat)	27.95(Lena)	29.01(Lena)	28.84 (Lena)	27.95(Lena)	28.59(Lena)	28.47(Lena)	27.40 (Lena)	29.3444 (Lena) 26.1193 (Boat)
90	25.4 (Lena) 21.5 (Bridge)	24.316 (Lena) 22.220 (Boat)	25.58(Lena)	26.04(Lena)	26.17(Lena)	25.54(Lena)	26.02(Lena)	25.94(Lena)	25.11 (Lena)	27.4923 (Lena) 24.3986 (Boat) 21.7225 (Bridge)

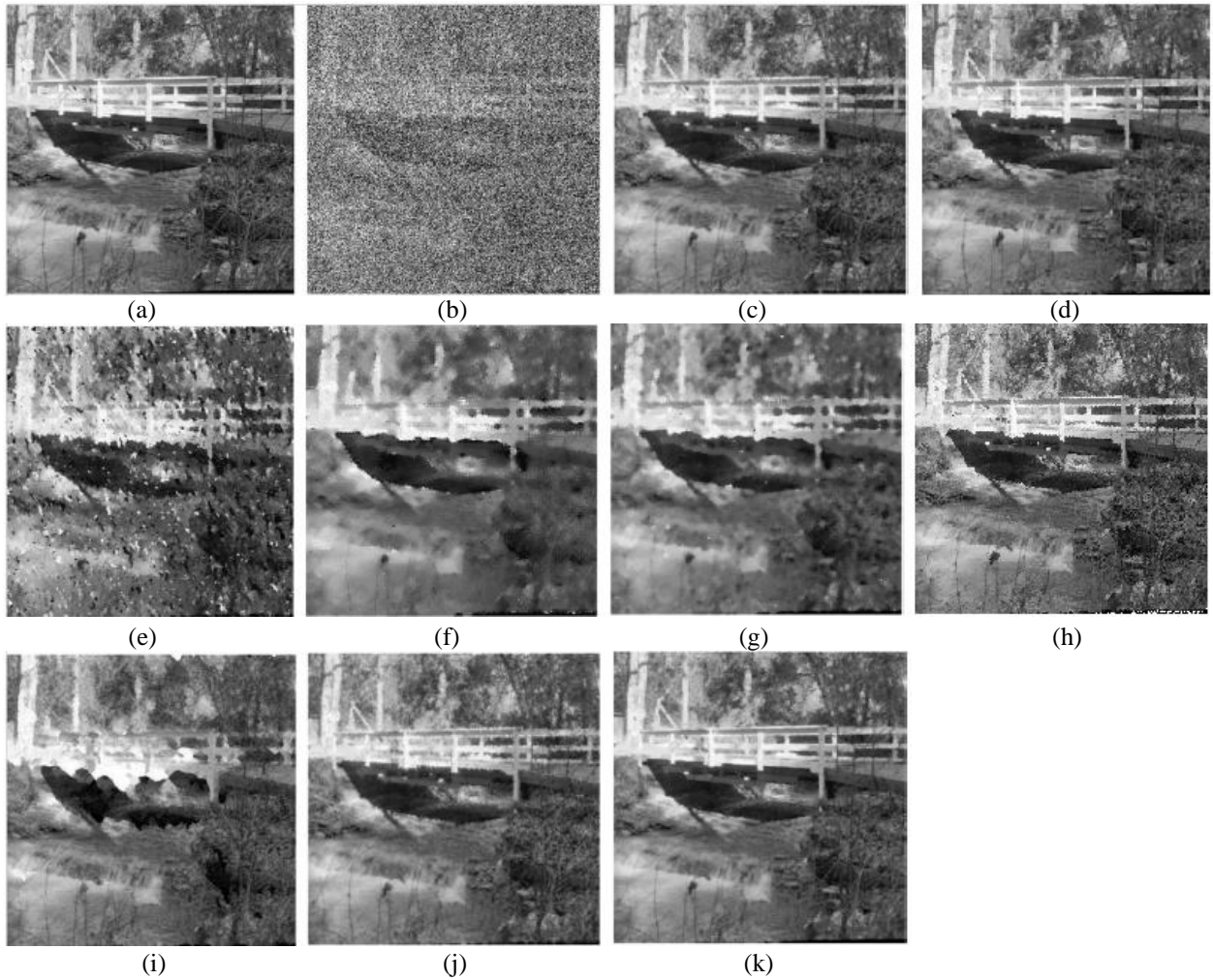


Fig. 8 (a) Original Boat image (b) image corrupted with salt and pepper noise (ND = 70%) (c) filtered image using fuzzy cell automata (d) ST MDF-AD (e) DDBSM (f) NASM (g) ISM (h) ITMF (i) PSM (j) Srinivasan (k) Chan et al

The edge preservation properties of the algorithm are appreciated at extreme levels of noise density when filtering the corrupted images. The failure of the other switching or decision-based filters is unavoidable as their limits become apparent at extreme high noise densities. The entropy guided threshold along with the energy minimization attributes of the proposed approach avoids successive smoothing in already treated regions with preserved edges, especially at high noise densities where differentiation between noise and signal becomes even more difficult to achieve in conventional schemes.

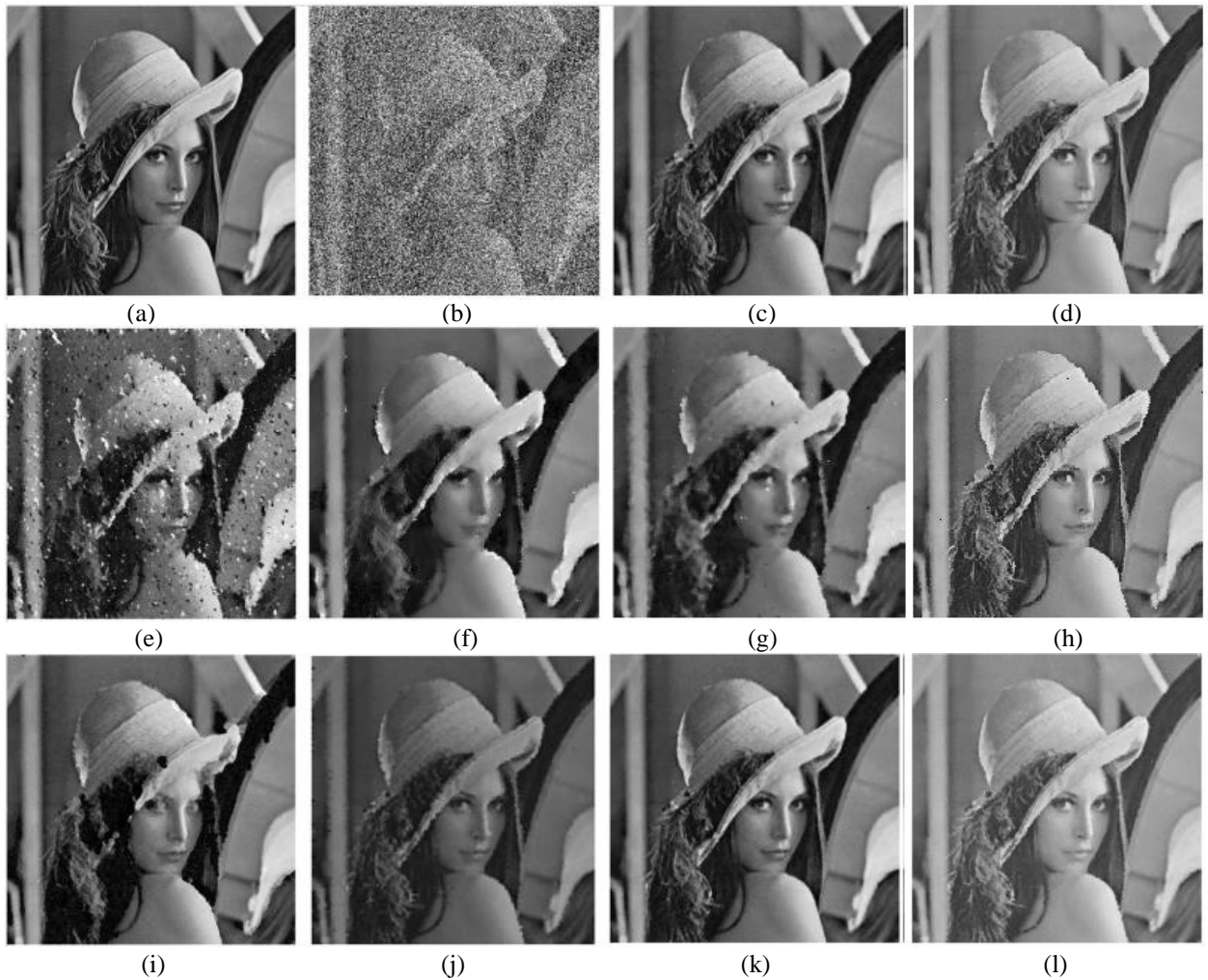


Fig. 9 (a) Original Boat image (b) image corrupted with salt and pepper noise (ND = 70%) (c) filtered image using fuzzy cell automata (d) STMDF-AD (e) DDBSM (f) NASM (g) ISM (h) ITMF (i) PSM (j) Srinivasan (k) Chan et al (l) Ching, et al

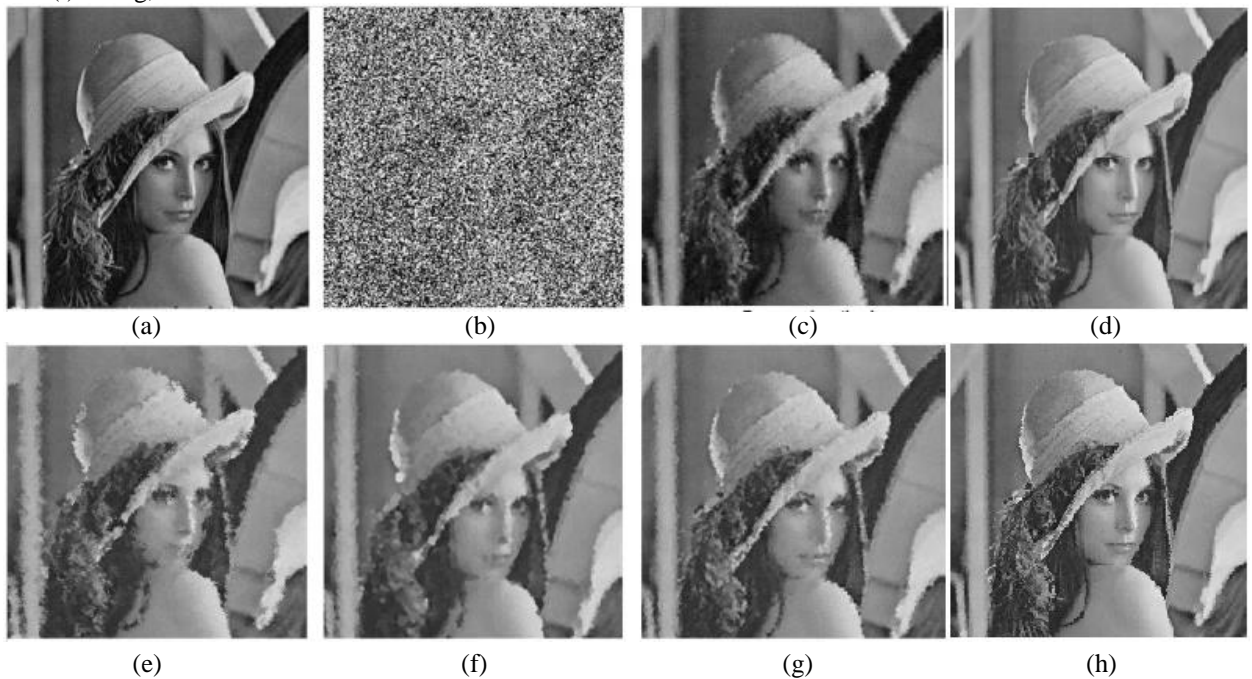


Fig. 10 (a) Original Boat image (b) image corrupted with salt and pepper noise (ND = 80%) (c) filtered image using fuzzy cell automata (d) STMDF-AD (e) Chan, et al (f) Srinivasan (g) Wang, et al (h) ITMF

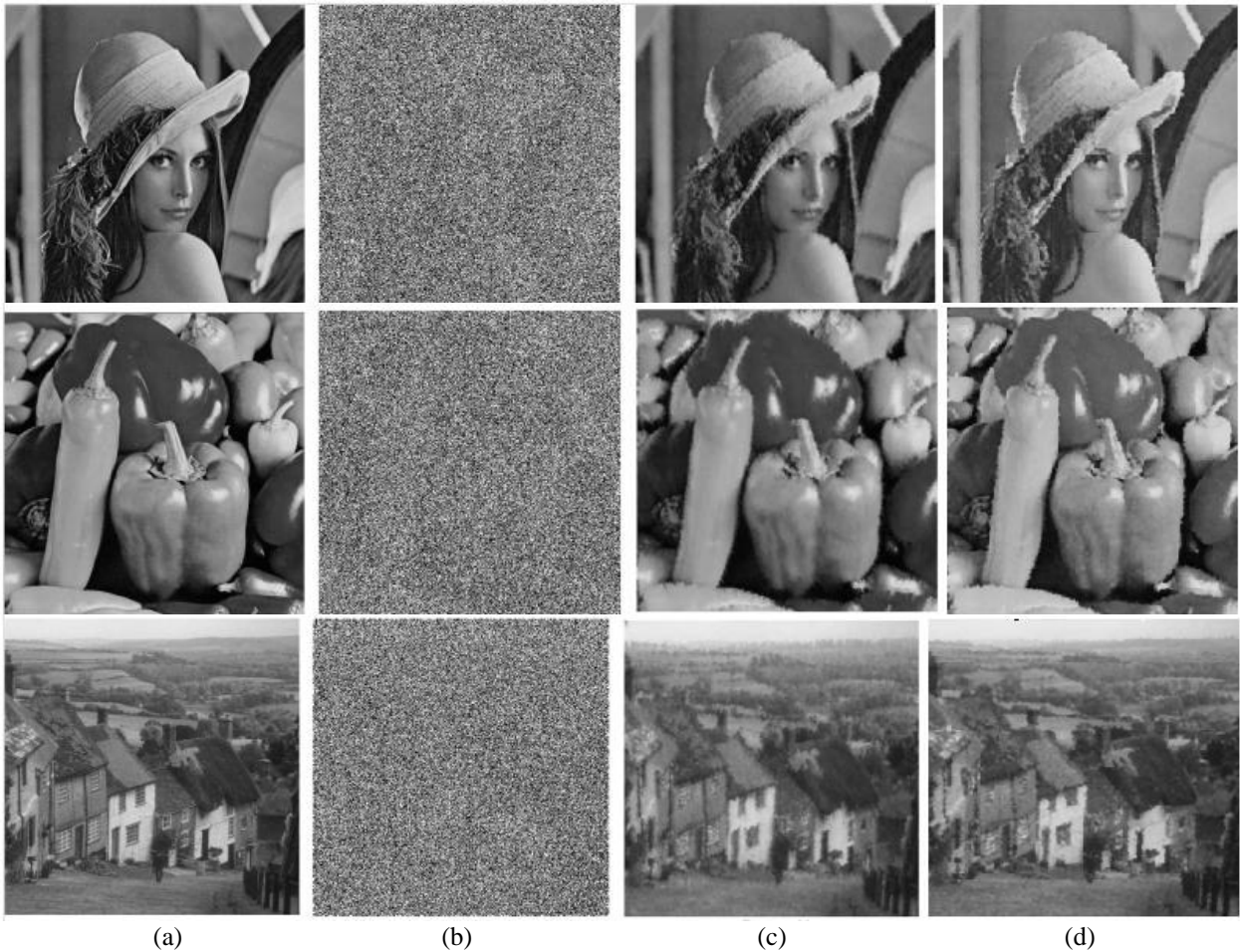


Fig. 11 (a) Original Lena, Peppers & Gold Hill images (b) images corrupted with salt and pepper noise (ND = 90%) (c) Filtered images using fuzzy cell automata (d) ST MDF-AD

4 Conclusion

This report has presented the theoretical considerations and detailed experimental results of the algorithm proposed in the paper titled, “Entropy-guided Switching Trimmed Mean-boosted Anisotropic Diffusion Filter [48]”. Other variations of the approach are also mentioned and will be treated in much more detail in future works.

References

- [1] R. C. Gonzalez and R. E. Woods, Digital Image Processing, 2nd edition, Prentice Hall, 2002.
- [2] R. C. Gonzalez, R. E. Woods and S. L. Eddins, Digital Image Processing Using MATLAB, Prentice Hall, 2004.
- [3] I. Pitas and A. N. Venetsanopoulos, "Order Statistics in Digital Image Processing," *Proc. IEEE*, vol. 80, no. 12, pp. 1893-1921, Dec. 1992.
- [4] P. Perona and J. Malik, "Scale-space and edge detection using anisotropic diffusion," *IEEE Transactions on Pattern Analysis and Machine Intelligence*, vol. 12, no. 7, pp. 629-639, 1990.
- [5] Z. Yang and M. D. Fox, "Speckle reduction and structure enhancement by multichannel median boosted anisotropic diffusion," *EURASIP Journal on Applied Signal Processing*, pp. 2492-2502, 2004.
- [6] L. Yin, R. Yang, M. Gabbouji and Y. Neuvo, "Weighted Median Filters: A Tutorial," *IEEE Trans. Circuits and Systems II: Analog and Digital Signal Processing*, vol. 43, pp. 157-192, March 1996.

- [7] H. Lin and A. N. Willson, "Median filter with adaptive length," *IEEE Trans. Circuits Syst.*, vol. 35, p. 675–690, June 1988.
- [8] H. Hwang and R. A. Haddad, "Adaptive median filters: New algorithms and results," *IEEE Trans. Image Process.*, vol. 4, no. 4, pp. 499–502, Apr. 1995.
- [9] G. Qiu, "An Improved Recursive Median Filtering Scheme for Image Processing," *IEEE Trans. Image Processing*, vol. 5, no. 4, April 1996..
- [10] G. Arce and J. Paredes, "Recursive Weighted Median Filters Admitting Negative Weights and Their Optimization," *IEEE Trans. Signal Processing*, vol. 48, no. 3, pp. 768-779, March 2000.
- [11] D. R. K. Brownrigg, "The weighted median filter," *Commun. Ass. Comput. Mach.*, vol. 27, no. 8, p. 807–818, Aug. 1984.
- [12] S.-J. Ko and S.-J. Lee., "Center weighted median filters and their applications to image enhancement," *IEEE Trans. Circuits Syst.*, vol. 38, p. 984–993, Sept. 1991.
- [13] Z. Wang and D. Zhang, "Progressive Switching Median Filter for the Removal of Impulse Noise from Highly Corrupted Images," *IEEE Trans. Circuits & Systems II: Analog and Digital Signal Processing*, vol. 46, no. 1, 1999.
- [14] K. K. Toh and N. A. M. Isa, "Noise Adaptive Fuzzy Switching Median Filter for Salt and Pepper Noise Reduction," *IEEE Signal Processing Letters*, vol. 17, no. 3, pp. 281-284, March 2010.
- [15] H.-L. Eng and K.-K. Ma, "Noise Adaptive Soft-Switching Median Filter," *IEEE Trans. Image Processing*, vol. 10, pp. 242-251, Feb. 2001.
- [16] E. E. Kerre and M. Nachtgal, *Fuzzy Techniques in Image Processing*, Physica-Verlag, 2000.
- [17] R. H. Chan, C.-W. Ho and M. Nikolova, "Salt-and-Pepper Noise Removal by Median-Type Noise Detectors and Detail-Preserving Regularization," *IEEE Trans. Image Processing*, vol. 14, pp. 242-251, October 2005.
- [18] Fabrizio Russo, "Fuzzy Filtering of Noisy Sensor Data," in *IEEE Instrumentation and Measurement Technology Conference*, pp. 1281- 1285, Brussels, Belgium,, June 4-6, 1996.
- [19] A. Restrepo and A. Bovik, "Adaptive Trimmed Mean Filters for Image Restoration," *IEEE Trans. Acoustics, Speech and Signal Processing*, vol. 36, no. 8, pp. 1326 - 1337, August 1988.
- [20] R. Oten and R. J. P. d. Figueiredo, "Adaptive Alpha-Trimmed Mean Filters Under Deviations From Assumed Noise Model," *IEEE Trans. Image Processing*, vol. 13, no. 5, pp. 627 - 639, May 2004.
- [21] T. Sun and Y. Neuvo, "Detail-preserving median based filters in image processing," *Pattern Recognit. Lett.*, vol. 15, p. 341–347, Apr. 1994.
- [22] E. Abreu, M. Lightstone, S. K. Mitra and K. Arakawa, "A new efficient approach for the removal of impulse noise from highly corrupted images," *IEEE Trans. Image Processing*, vol. 5, p. 1012–1025, June 1996.
- [23] Z. Wang and D. Zhang., "Restoration of impulse noise corrupted image using long-range correlation," *IEEE Trans. Signal Processing Lett.*, vol. 5, p. 4–8, Jan. 1998.
- [24] R. Garnett, T. Huegerich and C. Chui, "A Universal Noise Removal Algorithm With an Impulse Detector," *IEEE Trans. Image Processing*, vol. 14, pp. 1747-1754, Nov. 2005.
- [25] D. Florencio and R. Schafer, "Decision-based median filter using local signal statistics," in *Proc. SPIE Int. Symp. Visual Communications Image Processing*, Chicago, Sept. 1994.
- [26] D. Zhang and Z. Wang, "Impulse noise detection and removal using fuzzy techniques," *Electron. Lett.*, vol. 33, p. 378–379, Feb. 1997.
- [27] S. U., U. S. and S. F., "Salt and pepper noise filtering with fuzzy-cellular automata," *Journal of Computers and Electrical Engineering*, vol. 40, pp. 59-69, 2014.
- [28] S. Esakkirajan, T. Veerakumar, A. N. Subramanyam and C. H. PremChand, "Removal of High Density Salt and Pepper Noise Through Modified Decision Based Unsymmetric Trimmed Median Filters," *IEEE Signal Processing Letters*, Vols. 18, no. 5., no. 5, p. 287 – 290, May 2011.

- [29] Y. Jin, T. Ma, D. Guan, W. Yuan and C. Hou, "Review of applications of partial differential equations for image enhancement," *Scientific Research and Essays*, vol. 7, no. 44, pp. 3766-3783, 12 November 2012.
- [30] M. J. Black, G. Sapiro, D. H. Marimont and D. Heeger, "Robust anisotropic diffusion," *IEEE Transactions on Image Processing*, vol. 7, no. 3, pp. 421-432, 1998.
- [31] A. K. Sum and P. Y. Cheung, "IEEE International Conference on Acoustics, Speech and Signal Processing-Proceedings (ICASSP)," in *Stabilized anisotropic diffusion*, United States,, 2007.
- [32] J. W. Zhou and X. L. Liu, "The Fast Realization of the Robust P-M Model," *Microcomputing Information*, vol. 7 , pp. 199-201, 2011.
- [33] S. Osher and L. I. Rudin, "Feature-oriented image enhancement using shock filters," *SIAM Journal on Numerical Analysis*, vol. 27, no. 4 , pp. 919-940, 1990.
- [34] L. I. Rudin, S. Osher and E. Fatemi, "Nonlinear total variation based noise removal algorithms," *Physica D: Nonlinear Phenomena* , vol. 60 , no. 1, pp. 259-268, 1992.
- [35] P. Getreuer, "Rudin-Osher-Fatemi total variation denoising using split Bregman," *Image Processing On Line* , vol. 10, 2012.
- [36] P. Shanmugavadiva and P. S. E. Jeevaray, "Modified PDE-based Adaptive Two-Stage Median Filter for Images Corrupted with High Density Fixed Value Impulse Noise," *Trends in Computer Science Engineering Science*, vol. 204, pp. 376-383, 2011.
- [37] Z. Lu, W. Liu, D. Han and M. Zhang, "A PDE-based Adaptive Median Filter to process UV image generated by ICCD," *IEEE International Conference on Audio Language and Image Processing (ICALIP)*, pp. 543-546, 7-9 July 2014.
- [38] V. Saradhadevi and V. Sundaram, "An Adaptive Fuzzy Switching Filter for Images Corrupted by Impulse Noise," *Global Journal of Computer Science and Technology*, vol. 11, no. 4, March 2011.
- [39] A. Hussain, M. A. Jaffar, Z. Ul-Qayyum and A. M. Mirza, "Directional Weighted Median Based Fuzzy Filter For Random-Valued Impulse Noise," *ICIC Express Letters Part B: Applications ICIC International*, vol. 1, no. 1, pp. 9-14, Sept 2010.
- [40] V. Jayaraj and D. Ebenezer, "A New Switching-Based Median Filtering Scheme and Algorithm for Removal of High-Density Salt and Pepper Noise in Images," *EURASIP Journal on Advances in Signal Processing*, vol. 2010, p. 1–11, 2010.
- [41] Z. Deng, Z. Yin and Y. Xiong, "High probability impulse noise-removing algorithm based on mathematical morphology," *IEEE Signal processing Letters*, vol. 14, no. 1, pp. 31-34, 2007.
- [42] P. Y. Chen and C. Y. Lien., "An efficient edge-preserving algorithm for removal of salt and pepper noise," *IEEE Signal Processing Letters*, vol. 15, pp. 833-836, 2008.
- [43] X. Zhang and Y. Xiong, "Impulse noise removal using directional difference based noise detector and adaptive weighted mean filter," *IEEE Signal Processing Letters*, vol. 16, no. 4, pp. 295-298, 2009.
- [44] A. Jourabloo, A. H. Feghahati and M. Jamzad, "New algorithms for recovering highly corrupted images with impulse noise," *Scientia Iranica*, vol. 19, no. 6, pp. 1738-1745, 2012.
- [45] Z. Zhou, "Cognition and Removal of Impulse Noise with Uncertainty," *IEEE Transactions on Image Processing*, vol. 21, no. 7, pp. 3157-3167, 2012.
- [46] M.-H. Hsieh, F.-C. Cheng, M.-C. Shie and S.-J. Ruan, "Fast and efficient median filter for removing 1–99% levels of salt-and-pepper noise in images," *Engineering Applications of Artificial Intelligence*, vol. 26 , no. 4, pp. 1333-1338, 2013.
- [47] X. Jiang, "Iterated Truncated Arithmetic Mean Filter and Its Properties," *IEEE Transactions on Image Processing*, vol. 21, no. 4, p. 1537 – 1547, April 2012.
- [48] U. A. Nnolim, "Entropy-guided switching trimmed mean deviation-boosted anisotropic diffusion filter," *Journal of Electronic Imaging*, vol. 25, no. 4, pp. 1-15, July 08 2016.
- [49] Z. Y. Y. X. Z. Deng, "High probability impulse noise-removing algorithm based on mathematical morphology," *IEEE Signal Processing Letters*, vol. 14, no. 1, pp. 31-34, 2007.

